
Article:
Law, Richard orcid.org/0000-0002-5550-3567, Plank, Michael J. and Kolding, Jeppe (2016) Balanced exploitation and coexistence of interacting, size-structured, fish species. Fish and fisheries. pp. 281-302. ISSN 1467-2960

https://doi.org/10.1111/faf.12098

Balanced exploitation and coexistence of interacting, size-structured, fish species

Richard Law, Michael J. Plank, Jeppe Kolding

July 25, 2014

Alternative title: Coexistence of interacting fish species under balanced harvesting

Richard Law: York Centre for Complex Systems Analysis, Ron Cooke Hub, University of York, York YO10 5GE, UK

Michael J. Plank: School of Mathematics and Statistics, University of Canterbury, Christchurch, New Zealand

Jeppe Kolding: Department of Biology, University of Bergen, High Technology Center, P.O. Box 7800, N-5020 Bergen, Norway

Correspondence author: Richard Law: York Centre for Complex Systems Analysis, Ron Cooke Hub, University of York, York YO10 5GE UK. Tel +44 1904 325372; fax +44 1904 500159; email: richard.law@york.ac.uk

Running title: balanced harvest and species coexistence

Abstract

This paper examines some effects of exploitation on a simple ecosystem containing two interacting fish species, with life histories similar to mackerel (*Scomber scombrus*) and cod (*Gadus morhua*), using a dynamic, size-spectrum model. Such models internalize body growth and mortality from predation, allowing bookkeeping of biomass at a detailed level of individual predation and growth, and enabling scaling up to the mass balance of the ecosystem. Exploitation set independently for each species with knife-edge, size-at-entry fishing, can lead to collapse of cod. Exploitation to achieve a fixed ratio of yield to productivity across species can also lead to collapse of cod. However, harvesting balanced to the overall productivity of species in the exploited ecosystem exerts a strong force countering such collapse. If balancing across species is applied to a fishery with knife-edge selection, size distributions are truncated, changing the structure of the system, and reducing its resilience to perturbations. If balancing is applied on the basis of productivity at each body size as well as across species, there is less disruption to size structure, resilience is increased, and substantially greater biomass yields are possible. We note an identity between the body size at which productivity is maximized and the age at which cohort biomass is maximized. In our numerical results based on detailed bookkeeping of biomass, cohort biomass reaches its maximum at body masses less than 1 g, unlike standard yield-per-recruit models, where body growth and mortality are independent externalities, and cohort biomass is maximized at larger body sizes.

Keywords: balanced harvesting, ecosystem dynamics, productivity, resilience, size spectrum, yield-per-recruit

Contents

1 Introduction

Conventional heavy exploitation of aquatic ecosystems generates major disruption. Effects on the ecosystems include truncation of age- and size-structures (Rice and Gislason, 1996; Hsieh et al., 2010), reduction in large-bodied species (Guénette and Gascuel, 2012), destabilization of populations (Hsieh et al., 2010), discarding of unsuitable fish (Kelleher, 2005), and fisheries-induced evolution (Laugen et al., 2014). One obvious and incontestable response to this is to call for reduction in levels of exploitation. However, the importance of aquatic ecosystems to coastal and lake-margin communities around the world means that in many places human pressures on them are still likely to increase in the future.

Usually, the response to overfishing, collapsed stocks and fisheries-induced disruption is to try to improve the selectivity of fishing, to target more accurately the sizes and species needed for the market (COM, 2012). However, more careful targetting of large fish will disrupt size structure further, cause loss in resilience of stocks by reducing the abundance of large mature adults (Hsieh et al., 2010), and strengthen directional selection on life history traits potentially leading to faster fisheries-induced evolution. An alternative, motivated by ecological considerations, is to try to bring fishing closer in line with the natural productivity of components of aquatic ecosystems, the approach of so-called balanced harvesting (Zhou et al., 2010; Garcia et al., 2012). This is also selective, but there is an intuition that the overall effects of balanced harvesting should be less disruptive to the ecosystems themselves.

To go from an intuition about balanced harvesting to a firm foundation calls for quantitative analysis of exploitation patterns. Numerical analysis of balanced harvesting shows that it works well in preserving size structure, reducing the destabilizing effects of exploitation and, at the same time, increasing biomass yields, when applied to a single-species community living with a fixed plankton spectrum (Law et al., 2012, 2013). However, it is not clear how well it works in retaining a balance among species that live together and are coupled by body-size-dependent, predator-prey interactions. A recent study on generic behaviour of a multispecies community suggests the properties of preserving trophic structure and increasing biomass yields are retained (Jacobsen et al., 2014), but the detailed consequences of differ-

ent patterns of exploitation on the relative abundance and coexistence of interacting species are not known. In particular, the effect on coexistence of tuning fishing mortality species by species needs to be understood, as this is an important control measure for regulating multispecies aquatic ecosystems, such as those under the Convention for the Conservation of Antarctic Marine Living Resources (Miller and Slicer, 2014).

This paper examines how to organize exploitation of an aquatic ecosystem to maintain the balance of species, as well as to achieve sustainable yields from the species. As Jacobsen et al. (2014), we use dynamic size spectra, originally motivated by observed regularities in aggregated body size–abundance distributions of marine ecosystems (Sheldon and Parsons, 1967; Sheldon et al., 1972; Platt and Denman, 1978; Silvert and Platt, 1978), and readily disaggregated to describe the changing size distributions of interacting taxa (Andersen and Beyer, 2006; Hartvig et al., 2011; Hartvig and Andersen, 2013). Size-spectrum dynamics explicitly track biomass as it moves through the ecosystem (Persson et al., 2014): fish only grow as a consequence of eating other organisms, and predation is an important cause of death. This flow of biomass is at the heart of balanced harvesting because the balancing is set by natural productivity, i.e. the flow of biomass through the system, per unit volume, per unit time.

We take the simplest possible setting of two interacting fish species in which to examine the effects of fishing on the balance between species, with parameters set to approximate the life histories of mackerel (*Scomber scombrus*, Scombridae) and cod (*Gadus morhua*, Gadidae). Mackerel abundance was high in the N E Atlantic in 2013 (possibly the highest level ever recorded), and its exploitation and interaction with other species is the subject of international debate. Thus knowledge on how it might interact with other commercially important species is of particular interest at the present time. However, the basic ideas in this paper would readily transfer to other ecosystems dominated by a small number of fish species, such as those in the Baltic Sea (Möllmann et al., 2008).

2 Unexploited ecosystem at equilibrium

We start by describing the dynamics of an unexploited ecosystem, as this provides a template onto which different kinds of exploitation can be imposed and compared.

To obtain dynamics similar to mackerel and cod, asymptotic body masses were assumed to be 650 g for mackerel, and 30 kg for cod, with an egg mass 0.001 g for both species. Mackerel has an important empirical property of growing from an egg to over 100 g in its first year (Villamor et al., 2004), which was achieved by assuming a relatively large volume searched per unit time, greater than that of cod (Hunter, 1981). In addition, the planktivorous behaviour of mackerel (Olaso et al., 2005) was incorporated by a relatively large preferred predator-prey mass ratio, compared to cod's, so that it feeds on smaller organisms. Parameters are summarized in Table 1, and information on sources is in Appendix B.

2.1 Model

A dynamic, size-spectrum model was used, as set out in Appendix A. Such models explicitly couple growth (somatic and gonadic) to predation mortality. When sexual maturity is reached, incoming biomass is allocated increasingly to reproduction, the proportion reaching 1 at the asymptotic body mass. We focus on behaviour close to the equilibrium of the ecosystem. Knowledge of the equilibrium properties is helpful, but it is important to bear in mind that this is not the only state that matters, and we envisage this study as giving a basis on which more complicated nonequilibrium and seasonal analyses could be built.

Mackerel and cod were treated as separate spectra, supported by a fixed plankton spectrum. (The plankton can be thought of as having a much shorter time scale for their dynamics: see Appendix A, Eq. (A.13).) For simplicity, feeding was assumed to be indiscriminate across taxa. This means that, in keeping with observations, there was cannibalism, as well as predation on other taxa (Smith and Reay, 1991; Neuenfeldt and Köster, 2000; Hillgruber and Kloppmann, 2001; Robert et al., 2008). Feeding was assumed to depend on the prey's body size relative to the predator's, for consistency with empirical information (Jennings et al.,

2001). Thus prey size increased smoothly as the fish grew, and an ontogenetic shift in the feeding niche lies at the heart of the model (Werner and Gilliam, 1984; Rudolf and Lafferty, 2011). See Appendix A, Eq. (A.5) for the feeding-rate function.

Since cod grow larger than mackerel, the ecosystem might be thought of as a trophic chain in which cod feeds on mackerel. Such a construct is unwarranted: both species start at the same egg size, and small cod are a source of food for larger mackerel, as well as vice versa. In fact, mackerel were not able to persist under predation by cod in our model, when cod were excluded from their own diet. The two species do not separate cleanly into different trophic levels — to envisage the fish community as a simple food chain, would be to misconceive the way in which the ecosystem is organized.

2.2 Equilibrium states

With the parameters in Table 1, mackerel and cod coexisted at a stable equilibrium (leading real part of the eigenvalue of the Jacobian matrix: -0.17 y^{-1}). Note that dynamic size spectra have the feature of 'distributed' density-dependence, acting on body growth at all stages, as well as on mortality and reproduction. This greatly extends feedbacks (both positive and negative) beyond those assumed in standard stock-recruitment relations (Lorenzen and Enberg, 2002; Lorenzen, 2008), and beyond those in models that do not incorporate body growth. No stock-recruitment relation was imposed here (c.f. Jacobsen et al., 2014): all feedbacks acted internally through the size-dependent predation, and through the growth and reproduction that this feeding led to. This means that the relative abundances of the species were regulated directly by feeding and predation. It also avoided leakage of biomass from the ecosystem that would have had to be accounted for when examining mass flows (Section 2.6).

Both mackerel and cod also existed at stable equilibria in the absence of the other species (leading real parts of the eigenvalue of the Jacobians: -0.96, -0.44 y^{-1} for mackerel and cod subsystems respectively). This is unsurprising in the case of mackerel, since food from the plankton spectrum is sufficient to enable growth to maturity. However, the single-species

equilibrium for cod is more delicate. Cod need a 'trophic ladder' (Hartvig and Andersen, 2013) of smaller fish — they cannot get to maturity by consuming plankton alone. The trophic ladder could be supplied by mackerel or by small cod. Thus cod might establish itself in an ecosystem through a pre-existing population of mackerel. If mackerel was then wiped out for some reason, cod would remain in the ecosystem, mackerel only playing a catalytic role in community assembly (Law and Morton, 1996). Cod is vulnerable though: if its density for some reason was to fall sufficiently, growth to maturation through cannibalism would no longer be assured and renewal of the cod population would be threatened. This is an Allee effect (Hartvig and Andersen, 2013), as cod's equilibrium at zero density is an attractor as well as the equilibrium at positive density, and is one of a number of ways in which an Allee effect can emerge from predator-prey interactions (de Roos et al., 2003; van Kooten et al., 2005).

2.3 Departures from scale invariance

In an idealized setting of scale invariance, the equilibrium size spectra would be straight lines on a log-log plot (Benoît and Rochet, 2004). However, explicit life histories inevitably break scale invariance of the species size spectra, leading to departures from linearity at the species level (Fig. 1). The equilibrium size spectra (Fig. 1 a,b) had bumps at body sizes around maturation, where incoming food is transferred increasingly to reproduction as opposed to somatic growth. Scale invariance was also broken by the fixed egg size.

Another consequence of breaking scale invariance was that mass-specific growth rates and productivities no longer decreased linearly in parallel on a log-log plot as functions of body mass (Fig. 1 c,d) (Law et al., 2013). Mass-specific growth rates were still monotonic decreasing, but productivities had intermediate maxima. This is important because the shape of the productivity function provides one basis for balanced harvesting (Law et al., 2012, 2013), and the shape of the function also gives some insight into yield-per-recruit (YPR) methods traditionally used in fisheries management (Section 3.3).

2.4 Productivity

Note that productivity of species i is defined here as an integral over body size x of the product of individual body mass, abundance, and mass-specific growth rate (dimensions: M V^{-1} T^{-1}). Since incoming mass is partitioned between somatic growth and reproduction, the productivity comes in two parts:

$$\text{somatic: } P_i = \int \epsilon_i(x) g_i(x) u_i(x) w_0 e^x dx \tag{2.1}$$

$$\text{reproductive: } R_i = \int \big(1 - \epsilon_i(x)\big) g_i(x) u_i(x) w_0 e^x dx, \tag{2.2}$$

where w_0 is an arbitrary mass to scale from mass to log mass ($x = \log(w/w_0)$), $u_i(x)$ denotes the density of species i at body size x, and $g_i(x)$ is the mass-specific growth rate, of which a proportion $\epsilon_i(x)$ is channelled into somatic material and a proportion $1 - \epsilon_i(x)$ into reproduction.

2.5 Growth trajectories

The average growth trajectories from the model at equilibrium emerged simply as a result of feeding and growth, without imposing any explicit functional form (Fig. 1 e,f). Their resemblance to estimated von Bertalanffy growth functions for mackerel and cod (Villamor et al., 2004; Limburg et al., 2008) is expected, because we used reported functions to find appropriate volumes searched per unit time in the model. Nonetheless, the trajectory for mackerel captures properly its remarkably fast growth over its first year of life and its much slower growth subsequently, which the fitted von Bertalanffy function does not. Note that growth of cod benefits from the presence of mackerel.

2.6 Mass balance

At equilibrium, certain mass balances must be satisfied. The basic equality is that all mass losses from each species i must be balanced by corresponding gains (Balance 1):

$$P_i + R_i = D_i + D_{o,i} + Y_i + R_i/2, \tag{2.3}$$

with dimensions: $\mathrm{M\,V^{-1}\,T^{-1}}$ throughout (derived from integrals over body size at equilibrium in Appendix C). P_i is the productivity from somatic growth (Eq. 2.1), R_i is the productivity from mass flow to reproduction (Eq. 2.2), D_i is mass loss through predation, $D_{o,i}$ is the mass loss through natural mortality other than predation, and Y_i is mass loss due to fishing (used in the next section). The extra loss term $R_i/2$ comes from assuming that half the mass to reproduction is channelled through males, and that this is also lost.

Separate from Balance 1, all gains to the fish community from the plankton must be balanced at equilibrium by corresponding losses from the fish community. This gives Balance 2:

$$\sum_{i=1}^{n} \left(P_{i0} + R_{i0}\right) = \sum_{i=1}^{n} \left((1-K)\sum_{j=1}^{n} D_{ji} + D_{o,i} + Y_i + R_i/2\right), \tag{2.4}$$

where P_{i0}, R_{i0} are the productivity inputs to i from plankton, K is the food conversion efficiency (Table 1), D_{ji} is the mass loss to i from predation by j, and n is the number of fish species. Summing Balance 1 over all fish species and subtracting Balance 2 leaves a remaining balance that comes from recycling mass among fish. This is Balance 3:

$$\sum_{i=1}^{n}\sum_{j=1}^{n} \left(P_{ij} + R_{ij}\right) = K\sum_{i=1}^{n}\sum_{j=1}^{n} D_{ji}. \tag{2.5}$$

Further disaggregation of Balance 3 to pairwise interactions between species is not possible because, in general, interactions between species are not symmetric; for instance, one species might only be the prey of the other.

In the mackerel-cod system, the rate of mass flow from cod to mackerel was similar to the rate from mackerel to cod, at equilibrium (Fig. 2). Mackerel is as important a predator on

cod, as cod is on mackerel, which illustrates how misleading it is to think of these species as forming a trophic chain. However, mass flow through cannibalism was much greater in mackerel than in cod, because of the greater abundance of mackerel over the body-size range it feeds on (Fig. 1a,b). This means that the efficiency with which mackerel turns its production into cod food, its ecotrophic efficiency (Dickie, 1972), is rather low: $0.94/4.74 = 0.20$. Cod, with relatively little cannibalism, was more efficient at turning production into mackerel food: $0.78/0.94 = 0.83$. The transfer efficiency is the product of the ecotrophic efficiency and the food conversion efficiency (Dickie, 1972). Thus, with a food conversion efficiency $K = 0.2$ for both species (Table 1), cannibalism makes the transfer efficiency of turning mackerel biomass into cod biomass low (0.04), compared with that of turning cod biomass into mackerel (0.17). Balances (1), (2) and (3) (Eqns (2.3), (2.4), (2.5) respectively), were close to zero in both species, but not exact, because of the discretization needed to do the computation.

3 Exploiting the ecosystem

We examine harvesting at equilibrium, beginning with conventional, single-species management, where size-at-entry regulations are applied one species at a time, ignoring biological predator-prey interactions across species. From this starting point, we make two steps towards an ecosystem approach. The first is to find a balance across species that promotes their coexistence as fishing mortality increases, without taking into account the size-dependence of productivity. This is not a big step to make, as it is a matter of how to tune fishing mortality rates across species using whatever distribution of fishing over body size is already in place. The second step involves balancing across body size as well as across species. This is more demanding, but it should be considered because productivity changes greatly as fish get larger (see for instance Fig. 1 c,d).

These comparisons complement those made by Jacobsen et al. (2014). Their unbalanced harvesting patterns used a fixed fishing mortality rate for every species, whereas the single-species management here was designed to show some consequences of applying different

fishing mortalities that do not simultaneously allow for interactions between the species. Their balanced harvesting patterns were based on fixed, external, scaling assumptions about productivity, whereas here fishing was continually adjusted across species on the basis of information about productivity emerging from the current pattern of harvesting, until equilibrium was reached.

3.1 Single-species management

Here entry into the fishery was assumed to be knife-edged, starting at 100 g for mackerel and at 1000 g for cod, fishing mortality being the same at all larger body sizes. The fishing mortality rate was fixed for one species and altered for the other species, in keeping with a management regime focused on single species. In view of the high productivity of mackerel, the greatest sustainable biomass yield overall would be expected from eliminating cod. But we do not go into this, as it would not be in the spirit of conservation of the ecosystem. A maximum sustainable yield for a species is clearly contingent on the abundance of other species (its predators and prey), and cannot be decided in isolation.

The significant feature of the results (Fig. 3) is not the change in stock biomass and yield of the species in which fishing mortality is varied; rather it is the change in the species in which fishing mortality is fixed. Thus, in Fig. 3a, where fishing on cod was fixed at $F_c = 0.5$ y^{-1}, the cod biomass and yield were zero when fishing on mackerel was relatively light, as cod could not maintain a population under the combined adverse effects of mortality from harvesting and heavy predation from a large population of mackerel. The combination of abundant mackerel and heavy fishing on cod is evidently problematic for continued existence of cod. The biomass of mackerel decreased as it was fished harder, leading to less predation by mackerel on cod, and an increase in yield of cod. A benefit to cod of this kind has been noted following the collapse of herring stocks in the North Sea (Speirs et al., 2010); see also van Denderen and van Kooten (2013). For large enough F_m, however, the yield of cod started to decline again, because mackerel's other role as a source of food for large cod was jeopardized. This happened despite a continuing increase in biomass of cod, because smaller cod benefited from reduced predation by mackerel. To put it another way, cod's size spectrum responded

to the loss of mackerel in different ways at different body sizes.

In the reverse case (Fig. 3b), where fishing on mackerel was fixed at $F_m = 1.0\ \mathrm{y}^{-1}$, the mackerel yield increased monotonically with heavier fishing on cod, through the reduction of predation by cod on mackerel, until cod collapsed at about $F_c = 0.8\ \mathrm{y}^{-1}$. A similar effect of increasing F_c has been noted on sprat and herring in a recent multispecies assessment of the Baltic Sea (ICES, 2013c).

As is well understood in fisheries science (ICES, 2013b), it is difficult to manage a fishery at the ecosystem level by controlling fishing one species at a time, when species are coupled through predation. The effect of coupling is particularly obvious when the number of species is small. Increasing the number of species would dilute this effect, as would a reduction in the strength of coupling between the species.

3.2 Harvest balanced across species, not body size

An alternative to the single-species approach is to try to achieve a balance in fishing across species. 'Balancing' could be interpreted in a number of different ways – there is no general agreement on this (see Section 5). In any event, balancing across species can be done regardless of the way in which fishing is distributed over body sizes within species. So we continue with the size-at-entry fishery on mackerel and cod in Section 3.1, but instead of managing each species in isolation, we adjust fishing mortality to try to achieve a balance between them. There are many methods for doing this (Section 5), of which we investigate two here.

The first approach is to adjust the fishing mortality on each species to try to get a similar ratio Y_i/P_i of yield to productivity for each species. This was achieved by setting the fishing mortality according to $F_i = c_1 P_i / B_i^*$ (Appendix D, Eq. (D.3)), where c_1 is a dimensionless constant describing the overall intensity of fishing and B_i^* is the amount of biomass of species i in the fishery (i.e. individuals with body size greater than the size-at-entry). In this way, a small yield is taken from a species with low productivity and a large yield from one with high productivity. Fig. 4a shows Y against P, for each species, as the overall fishing intensity

c_1 is gradually increased. Because this fishing pattern guarantees that $Y_i/P_i = c_1$ for each species, the pairs of points in Fig. 4a lie on parallel lines of constant Y/P, moving up the graph as c_1 increases. However, the figure shows that, while the exploitation ratios Y_i/P_i were balanced across species, the productivities were not. As the fishing intensity increased, the productivity of mackerel increased slightly, while the productivity of cod crashed as the cod population collapsed.

A second, alternative approach, is simply to set fishing mortality in direct proportion to the productivity of the species, i.e. $F_i = c_2 P_i$ (Appendix D, Eq. (D.4)), where c_2 is a constant describing the overall intensity of fishing, in this case with dimensions V M^{-1} (Fig. 4b). This time, the pairs of points in Fig. 4b do not lie on parallel lines because the species no longer have the same exploitation ratios Y_i/P_i (the exploitation ratio for mackerel is roughly three times that of cod). Importantly, adjusting the fishing mortalities in tune with the current productivities kept the two species much better in balance up to levels of exploitation that would have caused collapse of cod in Fig. 4a.

3.3 Harvest balanced across species and body size

Fisheries that concentrate on large body sizes miss a substantial part of the productivity of aquatic ecosystems (Law et al., 2012, 2013). Here, we extend the approach in Section 3.2 to examine the effects of harvesting balanced by body size, as well as by species. A minimum body size for exploitation is still needed, and we set this at 1 g.

In doing this, we point out the following formal connection between (a) harvesting by size-dependent productivity, and (b) harvesting to maximize YPR within cohorts of individuals. For a species at equilibrium, there can exist one (or more) body size x^* with the following three properties: (a) it gives a maximum productivity with respect to body size x; (b) it gives a maximum biomass for a cohort with respect to age; (c) it achieves equality between the mass-specific growth rate and total death rate (Hillis and Arnason, 1995; Houde, 1997). (See Appendix E for an explanation.) Hence, the messages from YPR models and from balanced harvesting are actually quite similar. YPR sets fishing to start near the biomass peak of the

cohort, and equivalently, balanced harvesting sets fishing to be greatest at the productivity peak, which occurs at the same age and body size. The key difference between x^* from biomass bookkeeping in size-spectra models, and x^* from standard YPR models with growth uncoupled from mortality, is numeric: in the example in this paper for instance, x^* occurs at body sizes < 1 g (see Section 5).

As in Section 3.2, in the absence of agreement as to what exactly it means to balance exploited species, we consider two of many possible options. The first makes fishing mortality proportional to the mass-specific, somatic growth rate of individuals of species i and body size x, i.e. $\mu_{f,i}(x) = c\epsilon_i(x)g_i(x)$ (Appendix D, Eq. (D.5)), where c is a dimensionless constant describing the overall intensity of fishing (Fig. 5). This is consistent with the notion of productivity suggested for balanced harvesting in Note 8 of Garcia et al. (2012), at least so far as dimensions are concerned. Balancing now applies across species and at every harvested body size because, at equilibrium, the exploitation rate is scaled throughout by the same value c. The outcome is that the species have the same ratio Y_i/P_i^*, where P_i^* is the productivity in the harvested size range. For comparability with the other figures we use P_i, the productivity over all body sizes, so in fact the pairs of points in Fig. 5a lie approximately, but not exactly, on parallel lines. However, as in Fig. 4a, cod collapsed as the overall fishing intensity increased, and the productivity of mackerel increased as this happened (Fig. 5a). At the point of elimination of cod, the ecosystem productivity was close to 120 % of its virgin value, because the inefficient transfer of biomass to cod was removed, and mackerel was being harvested at less than 50 % of its single-species MSY level. Hence, setting fishing in proportion to the mass-specific, somatic growth rate does not maintain a desirable balance of species.

A second, alternative approach is to set fishing in proportion to productivity at every body size in both species, as defined in terms inside the integral of Eq. (2.1), i.e. $\mu_{f,i}(x) = cp_i(x)$, where c is a constant describing the overall intensity of harvesting with dimensions V M^{-1}, and $p_i(x)$ is the productivity of species i at body size x (Fig. 5b) (Appendix D, Eq. (D.7)). This exploitation pattern held the species in balance better than exploitation in proportion to the mass-specific growth rate (compare with Fig. 5a). Pairs of points corresponding to each

fishing intensity c do not lie on lines of constant Y/P, and low levels of fishing in particular show greater Y_i/P_i ratios emerging for mackerel than for cod. The species coexisted until exploitation brought the total ecosystem productivity down to about 30 % of its virgin value. The yields were also substantially greater than those in Fig. 4b, as the high productivity at small body sizes was better exploited.

4 Conservation and sustainable exploitation

Harvesting exerts a strong force countering the loss of species under exploitation, when set in balance with the overall productivity of each species in the exploited ecosystem. The per capita fishing rate rises as productivity increases so that a single species does not come to dominate the system, and it falls as productivity decreases so that rare species are protected. It acts as a form of intraspecific, density-dependent mortality that introduces a negative feedback. This diversity-maintaining effect of balanced harvesting can be seen in Fig. 4b and 5b.

Effects on the shape of species size spectra are more intricate, because fishing has indirect, as well as direct, effects on the spectra. To illustrate this, Fig. 6 compares the spectra from the contrasting patterns of fishing in Section 3, after the total biomass at equilibrium has been brought down to approximately 0.75 of its unharvested value. (Cod was absent at this biomass in Fig. 4a, 5a, and it is coincidental as to whether there is coexistence for a given F_m, F_c pair in a standard, size-at-entry fishery, so we consider only the fishing patterns in Fig. 4b, 5b.) As expected, there was truncation of the size structure in the size-at-entry fishery with balancing across species (Fig. 6a), because such fishing was still focused on large individuals. However there was also some truncation in the cod spectrum when balancing was across body size as well as species (Fig. 6b), though less than in Fig. 6a. This was an indirect consequence, rather than a direct effect of fishing mortality, because fishing reduced the food available for large cod, and they grew more slowly. Notice that, despite the fact that cod was generating yield, its abundance rose above its unexploited level, as a result of the strong equalizing force of balanced harvesting.

Truncation of age structure in size-at-entry fisheries destabilizes the mackerel-cod ecosystem, just as it is known to do in single-species analyses (Law et al., 2012): coupling the dynamics of two species does not remove the instability (Fig. 7). This figure includes a conventional size-at-entry fishery, with fishing mortality on mackerel twice that on cod, these mortalities being increased proportionately up to a value at which cod was eliminated. The real part of the leading eigenvalue (a measure of instability) increased as fishing was made more intense, eventually becoming positive and destabilizing the ecosystem. A similar change was evident when exploiting a size-at-entry fishery with balancing across species. It was only under full balancing across body size as well as species that the system remained resilient, the eigenvalue becoming more negative until fishing mortality was large. We interpret this difference as an outcome of more big old fish being present under full balanced harvesting, spreading reproduction over a longer adult life.

Consistent with the maintenance of a greater stock of big old fish are the tails of the survivorship curves of cohorts in Fig. 8. Although the size spectrum of cod was truncated under full balancing (Fig. 6b), evidently this was because cod grew more slowly, not because old fish were absent. It is notable how much closer to the unexploited ecosystem the survivorships were when fishing was balanced across body size as well as species. This implies that fishing mortality was to some extent replacing natural mortality, rather than adding to it (Law et al., 2013). Harvesting some large fish releases their prey from predation; these prey are then available for harvesting, as are their prey, and so on. When balanced across body size, harvesting evidently keeps the combined mortality from fishing + predation relatively close to predation mortality in the absence of fishing. Such replacement may underly the relatively benign effects of exploitation, when in balance with productivity at body size and across species.

5 Discussion

Our results demonstrate that harvesting, when held in balance with productivity, is potentially a strong force preventing collapse of exploited species. This applies both when effects

of body size are ignored and when effects of body size are taken into account. Note that the term 'productivity' follows its normal usage in ecosystem ecology as a mass per unit volume (area) per unit time, i.e. with dimensions M V^{-1} T^{-1} (see of Eq. (2.1)), rather than a mass-specific rate (dimensions: T^{-1}) (Garcia et al., 2012). The amount of mass in the species matters as much as the per-unit-mass rate at which it is increasing when setting fishing mortality. Importantly, productivity was measured at the time of harvesting, so fishing mortality tracked and responded to the current productivity of exploited species. This is in contrast to previous work which drew on external information either about an unharvested ecosystem (Law et al., 2012, 2013), or an external scaling law (Jacobsen et al., 2014). Adaptive fishing of the kind used here calls for information on how fast fish are growing, readily available from size-at-age data, and stock abundance (available from fishery surveys, and catch per unit effort), disaggregated to the appropriate level.

There is no generally accepted notion of what it means to achieve a balance between species under exploitation. We tested a few of the many possibilities, and do not claim to have found the best answer. For instance, one could maintain the same ratio for biomasses or productivities of the species as in an unexploited system. However, productivity is a natural choice where exploitation of an ecosystem is concerned, and is at the heart of current discussions about balanced harvesting. Note that the size spectra of mackerel and cod were pulled towards each other under full balancing across body size and species (Fig. 6), making the species more even; in fact balanced harvesting made cod more abundant than it would have been in the absence of exploitation. We conjecture that full balancing by productivity has the potential to increase biodiversity above that of an unexploited ecosystem; this could be seen as interference with its natural structure. Other results from body-size balancing remain broadly similar to those observed previously (Law et al., 2012, 2013; Jacobsen et al., 2014), namely, generating greater biomass yields, increased system resilience, and enabling more substitution of natural mortality by fishing mortality.

A feature of balancing by productivity was an emergent exploitation ratio Y_i/P_i for mackerel greater than that for cod. We interpret this as an outcome of mackerel's especially rapid growth when small. It has been suggested that, in a simple food chain, exploitation rates on

intermediate species should be lower than on top species, so that some part of the biomass of intermediate species is kept in place to support species higher up the food chain (Kolding, 1993). However, as trophic levels become blurred through cannibalism and reciprocal predation, it seems that a greater exploitation rate is needed on the smaller, more productive species. Otherwise the abundant smaller species (here mackerel) drives down the larger species (here cod) by heavy predation, and this is deleterious to the yield from the larger species. It should be kept in mind though, that this could be context specific, being caused here by mackerel's especially fast somatic growth in its first year.

Fisheries science has a rule of thumb of setting fishing mortality of different species in proportion to their natural mortalities. However natural mortality is a moving target, because it depends on fishing mortality: for instance, heavier exploitation reduces stock density, which reduces cannibalism and predation on other species. It also leaves open the question as to what natural mortality should be used, as this mortality varies greatly across age and body size. An aggregate measure of natural mortality based on a ratio of productvity to biomass might be used, to which fishing mortality could be matched (as in Figure 4a), but this would not promote coexistence of exploited species according to our results.

The formal equivalence of the body size maximizing (a) productivity and (b) cohort biomass, bring together balanced-harvesting and conventional YPR approaches. In doing this, a remarkable divergence emerges from the calculations. On one hand, our calculations on mackerel and cod give maximum productivities at body masses less than 1 g. On the other hand, minimum legal landing sizes of these species in the European Union, underpinned by a number of factors including cohort biomass, are currently 20 to 30 cm for mackerel, and 30 to 35 cm for cod. This points to an important lack of understanding as to how mass flows through marine ecosystems. We illustrate the problem in Fig. 9, in which cohort biomass emerging from our unexploited equilibrium ecosystem is plotted with the mass-specific growth rate and total death rate. As expected from the productivities with their maxima at body sizes less than 1 g (Fig. 1c,d), maximum cohort biomasses (where the rate curves first intersect) occur shortly after egg hatching. In the case of cod there is a second small maximum at about age 4 y, as there are two further intersections of its rate functions. (We have not

dealt with an intersection at the very early larval stage (Houde, 1997), but would not expect this to have major effect on subsequent behaviour.) Notice that, if the natural death rate is not known and is replaced by an arbitrary value, say 1 y^{-1}, the intersection occurs at an age greater than 1 y, leading to the prediction that cohort biomass would not be maximized until the fish are considerably older. In doing this, however, the much higher mortality rate of fish within the first year is not being taken into account.

Obviously there are assumptions built into the feeding behaviour of fish in our model. However, we have done the mass balancing in more detail than previous work, starting with individual growth, and working through population dynamics, up to the ecosystem level (Persson et al., 2014). Among the other main multispecies approaches (Plagányi, 2007), ATLANTIS comes nearest to doing this (Horne et al., 2010), but, with disaggregation of prey already taken down to species, it does not deal with additional complications of mass flow from continuous body-size distributions of prey into the growth of predators. ECOSIM does biomass balancing, but aggregates over body size, often focusing on adults of species, prior to computation of mass flows, and does not deal with the continuous growth of organisms (Walters et al., 1997). OSMOSE disaggregates species by age, and uses an external function for body growth, modified by food availability (Shin and Cury, 2004). Gadget disaggregates by species, body size and area, and uses external information on body growth (Begley and Howell, 2004). The ecosystem approach adopted by ICES in the North Sea (ICES, 2013b) estimates the size-dependent predation mortality across species from a stochastic multispecies size-dependent food selection model (SMS) (Lewy and Vinther, 2004) but does not deal with the consequences for body growth. The challenge the standard YPR calculation faces is to find enough food in the ecosystem to achieve the observed growth of fish without increasing natural mortality; otherwise the body size at which cohort biomass is maximized will typically become smaller when mortality is accounted for. This needs investigation.

As Jacobsen et al. (2014) point out, the economic value of small fish is low in major commercial fisheries. However, size structures and resilience are being damaged in the ecosystems that support these fisheries (Rice and Gislason, 1996; Hsieh et al., 2010), and strong directional selection on genetic variation in life-history traits is being generated (Sharpe and

Hendry, 2009). Conservation calls for a change in approach, as does an ecosystem approach under the code of conduct of responsible fisheries (Garcia and Cochrane, 2005), even if economics do not. In addition, economic arguments for not catching small fish do not apply to the small-scale fisheries that employ most of the World's fishers (Mills et al., 2011; Kolding et al., 2014). It is a matter of particular concern that exploitation of small fish is actively discouraged in parts of the developing world where there is serious poverty, because of a management agenda from the developed world focused on harvesting large fish (Kolding and van Zwieten, 2011). Both food production and conservation stand to benefit from more balanced harvesting across body sizes, according to the results emerging from size-spectra models.

We make no claim that harvesting, when balanced by productivity across body size and species, is a general answer to the exploitation of aquatic ecosystems. But our numerical results suggest it does have several useful properties. Fishing, when set to current productivity of species, is a powerful force promoting species coexistence. In addition, fishing when set to productivity across body size, allows biomass yields to be increased, truncation of size and age structure to be reduced, and resilience of aquatic ecosystems to be increased.

Acknowledgements

We thank Arild Folkvord for advice on growth of fish larvae, and K. H. Andersen, S. Jennings and S. Zhou for commenting on this work. The School of Mathematics and Statistics, University of Canterbury NZ facilitated the research by hosting visits for RL. The research was supported by a RSNZ Marsden Grant, number 08-UOC-034.

References

Andersen, K. H. and Beyer, J. E. (2006). Asymptotic size determines species abundance in the marine size spectrum. *American Naturalist*, 168:54–61.

Begley, J. and Howell, D. (2004). An overview of Gadget, the Globally applicable Area-Disaggregated General Ecosystem Toolbox. ICES CM 2004/FF:13. pp 15.

Benoît, E. and Rochet, M.-J. (2004). A continuous model of biomass size spectra governed by predation and the effects of fishing on them. *Journal of Theoretical Biology*, 226:9–21.

Blanchard, J. L. (2008). *The dynamics of size-structured ecosystems*. PhD thesis, University of York.

Chambers, R. C. and Waiwood, K. G. (1996). Maternal and seasonal differences in egg sizes and spawning characteristics of captive Atlantic cod, *Gadus morhua*. *Canadian Journal of Fisheries and Aquatic Sciences*, 53:1986–2003.

COM, E. (2012). *Proposal for a Regulation of the European Parliament and of the Council on the Common Fisheries Policy General approach.* Council of the European Union, Brussels, 13 June 2012, Interinstitutional, File:2011/0195 (COD), 11322/12, PECHE 227.

Coombs, S. H. (1981). A density-gradient column for determining the specific gravity of fish eggs, with particular reference to eggs of the mackerel *Scomber scombrus*. *Marine Biology*, 63:101–106.

Datta, S., Delius, G. W., and Law, R. (2010). A jump-growth model for predator-prey dynamics: derivation and application to marine ecosystems. *Bulletin of Mathematical Biology*, 72:1361–1382.

Datta, S., Delius, G. W., Law, R., and Plank, M. J. (2011). A stability analysis of the power-law steady state of marine size spectra. *Journal of Mathematical Biology*, 63:779–799.

de Roos, A. M., Persson, L., and Thieme, H. R. (2003). Emergent Allee effects in top predators feeding on structured prey populations. *Proceedings of the Royal Society London B*, 270:611–618.

561 Dickie, L. M. (1972). Food chains and fish production. International Commission for the
562 Northwest Atlantic Fisheries Special Publications, No 8. 201–219.

563 Garcia, S. M. and Cochrane, K. L. (2005). Ecosystem approach to fisheries: a review of
564 implementation guidelines. *ICES Journal of Marine Science*, 62:311–318.

565 Garcia, S. M., Kolding, J., Rice, J., Rochet, M.-J., Zhou, S., Arimoto, T., Beyer, J. E.,
566 Borges, L., Bundy, A., Dunn, D., Graham, N., Hall, M., Heino, M., Law, R., Makino, M.,
567 Rijnsdorp, A. D., Simard, F., and Smith, A. D. M. (2012). Reconsidering the consequences
568 of selective fisheries. *Science*, 335:1045–1047.

569 Glazier, D. S. (2009). Activity affects intraspecific body-size scaling of metabolic rate in
570 ectothermic animals. *Journal Comparative Physiology B*, 179:821–828.

571 Guénette, S. and Gascuel, D. (2012). Shifting baselines in European fisheries: the case of
572 the Celtic Sea and Bay of Biscay. *Ocean and Coastal Management*, 70:10–21.

573 Hartvig, M. and Andersen, K. H. (2013). Coexistence of structured populations with size-
574 based prey selection. *Theoretical Population Biology*, 89:24–33.

575 Hartvig, M., Andersen, K. H., and Beyer, J. E. (2011). Food web framework for size-
576 structured populations. *Journal of Theoretical Biology*, 272:113–122.

577 Hillgruber, N. and Kloppmann, M. (2001). Small-scale patterns in distribution and feeding
578 of Atlantic mackerel (*Scomber scombrus* L.) larvae in the Celtic Sea with special regard to
579 intra cohort cannibalism. *Helgoland Marine Research*, 55:135–149.

580 Hillis, J. P. and Arnason, R. (1995). Why fisheries cannot be managed by technical measures
581 alone: a comparison of selected fisheries inside and outside the European Union. *ICES*
582 *CM 1995*, S/9.

583 Horne, P. J., Kaplan, I. C., Marshall1, K. N., Levin, P. S., Harvey, C. J., Hermann, A. J.,
584 and Fulton, E. A. (2010). Design and parameterization of a spatially explicit ecosystem
585 model of the Central California Current. Technical report, NMFS-NWFSC-104, National
586 Oceanic and Atmospheric Administration.

Houde, E. D. (1997). In Chambers, R. C. and Trippel, E. A., editors, *Early life history and recruitment in fish populations*, chapter 6. Patterns and consequences of selective processes in teleost early life histories, pages 172–196. Chapman and Hall, London.

Hsieh, C.-H., Yamauchi, A., Nakazawa, T., and Wang, W.-F. (2010). Fishing effects on age and spatial structures undermine population stability of fishes. *Aquatic Sciences*, 72:165–178.

Hunter, J. R. (1981). Feeding ecology and predation of marine larvae. In Lasker, R., editor, *Marine fish larvae: morphology ecology and relation to fisheries*, pages 34–77. University of Washington Press, Seattle.

ICES (2013a). 04 WGWIDE Report - Section 02 Northeast Atlantic Mackerel. Technical report, International Council for the Exploration of the Sea.

ICES (2013b). Advice note: Multispecies considerations for the North Sea stocks. Technical report, International Council for the Exploration of the Sea, Copenhagen, Denmark.

ICES (2013c). Report of the benchmark workshop on baltic multispecies assessments (wkbalt), 48 february 2013. Technical report, International Council for the Exploration of the Sea, Copenhagen, Denmark.

Jacobsen, N. S., Gislason, H., and Andersen, K. H. (2014). The consequences of balanced harvesting of fish communities. *Proceedings of the Royal Society B*, 281:20132701.

Jennings, S., Pinnegar, J. K., Polunin, N. V. C., and Boon, T. W. (2001). Weak cross-species relationships between body size and trophic level belie powerful size-based trophic structuring in fish communities. *Journal of Animal Ecology*, 70:934–944.

Kelleher, K. (2005). Discards in the world's marine fisheries. An update. Technical report, Fisheries Technical Paper No. 470, FAO Rome, 131 pp.

Killen, S. S., Costa, I., Brown, J. A., and Gamper, A. K. (2007). Little left in the tank: metabolic scaling in marine teleosts and its implications for aerobic scope. *Proceedings of the Royal Society B*, 274:431–438.

Kolding, J. (1993). Trophic interrelationships and community structure at two periods of Lake Turkana, Kenya: a comparison using the ECOPATH II box model. In Christensen, V. and Pauly, D., editors, *Trophic Models of Aquatic Ecosystems*, pages 116–123. ICLARM Conference Proceedings 26.

Kolding, J., Béné, C., and Bavinck, M. (2014). In Garcia, S., Rice, J., and Charles, A., editors, *Governance for Marine Fisheries and Biodiversity Conservation. Interaction and coevolution*, chapter 22 Small-scale fisheries - importance, vulnerability, and deficient knowledge. Wiley-Blackwell.

Kolding, J. and van Zwieten, P. A. (2011). The tragedy of our legacy: how do global management discourses affect small scale fisheries in the South? *Forum for Development Studies*, 38:267–297.

Laugen, A. T., Engelhard, G. H., Whitlock, R., Arlinghaus, R., Dankel, D. J., Dunlop, E. S., Eikeset, A. M., Enberg, K., Jørgensen, C., Matsumura, S., Nussle, S., Urbach, D., Baulier, L., Boukal, D. S., Ernande, B., Johnston, F. D., Mollet, F., Pardoe, H., Therkildsen, N. O., Uusi-Heikkila, S., Vainikka, A., Heino, M., Rijnsdorp, A. D., and Dieckmann, U. (2014). Evolutionary impact assessment: accounting for evolutionary consequences of fishing in an ecosystem approach to fisheries management. *Fish and Fisheries*, 15:65–96.

Law, R., Kolding, J., and Plank, M. J. (2013). Squaring the circle: reconciling fishing and conservation of aquatic ecosystems. *Fish and Fisheries*.

Law, R. and Morton, R. D. (1996). Permanence and the assembly of ecological communities. *Ecology*, 77:762–775.

Law, R., Plank, M. J., and Kolding, J. (2012). On balanced exploitation of marine ecosystems: results from dynamic size spectra. *ICES Journal of Marine Science*, 69:602–614.

Lewy, P. and Vinther, M. (2004). A stochastic age-length-structured multispecies model applied to north sea stocks. ICES CM 2004/FF:13. pp 33.

Limburg, K. E., Walther, Y., Hong1, B., Olson, C., and Stora, J. (2008). Prehistoric versus

639 modern Baltic sea cod fisheries: selectivity across the millennia. *Proceedings of the Royal*
640 *Society London B*, 275:2659–2665.

641 Lorenzen, K. (2008). Fish population regulation beyond stock and recruitment: the role of
642 density-dependent growth in the recruited stock. *Bulletin of Marine Science*, 83:181–196.

643 Lorenzen, K. and Enberg, K. (2002). Density-dependent growth as a key mechanism in the
644 regulation of fish populations: evidence from among-population comparisons. *Proceedings*
645 *of the Royal Society London B*, 269:49–54.

646 Mendiola, D., Alvarez, P., Cotano, U., Etxebeste, E., and de Murguia, A. M. (2006). Effects
647 of temperature on development and mortality of Atlantic mackerel fish eggs. *Fisheries*
648 *Research*, 80:158–168.

649 Miller, D. G. and Slicer, N. M. (2014). In Garcia, S., Rice, J., and Charles, A., editors, *Gov-*
650 *ernance for Marine Fisheries and Biodiversity Conservation. Interaction and coevolution*,
651 chapter 18 CCAMLR and Antarctic conservation: the leader to follow? Wiley-Blackwell.

652 Mills, D. J., Westlund, L., de Graaf, G., Kura, Y., Willman, R., and Kelleher, K. (2011).
653 In Pomeroy, R. S. and Andrew, N. L., editors, *Small-scale Fisheries Management*, chapter
654 1 Under-reported and Undervalued: Small-scale Fisheries in the Developing World, pages
655 1–15. CAB International.

656 Möllmann, C., Müller-Karulis, B., Kornilovs, G., and St John, M. A. (2008). Effects of
657 climate and overfishing on zooplankton dynamics and ecosystem structure: regime shifts,
658 trophic cascade, and feedback loops in a simple ecosystem. *ICES Journal of Marine*
659 *Science*, 65:302–310.

660 Neuenfeldt, S. and Köster, F. W. (2000). Trophodynamic control on recruitment success in
661 baltic cod: the influence of cannibalism. *ICES Journal of Marine Science*, 57:300–309.

662 Olaso, I., Gutiérrez, J. L., Villamor, B., Carrera, P., Valdés, P. L., and Abaunza, P. (2005).
663 Seasonal changes in the north-eastern Atlantic mackerel diet (*Scomber scombrus*) in the
664 north of Spain (ICES Division VIIIc). *Journal of the Marine Biological Association U.K.*,
665 85:415–418.

Persson, L., Van Leeuwen, A., and De Roos, A. M. (2014). The ecological foundation for ecosystem-based management of fisheries: mechanistic linkages between the individual-, population-, and community-level dynamics. *ICES Journal of Marine Science*, doi:10.1093/icesjms/fst231.

Plagányi, É. E. (2007). Models for an ecosystem approach to fisheries. FAO Fisheries Technical Paper 477, 108 pp, Food and Agriculture Organization of the United Nations, Rome.

Platt, T. and Denman, K. (1978). The structure of pelagic marine ecosystems. *Journal du Conseil International pour l'Exploration de la Mer*, 173:60–65.

Rice, J. and Gislason, H. (1996). Patterns of change in the size spectra of numbers and diversity of the North Sea fish assemblage, as reflected in surveys and models. *ICES Journal of Marine Science*, 53:1214–1225.

Robert, D., Castonguay, M., and Fortier, L. (2008). Effects of intra- and inter-annual variability in prey field on the feeding selectivity of larval Atlantic mackerel (*Scomber scombrus*). *Journal of Plankton Research*, 30:673–688.

Rudolf, V. H. W. and Lafferty, K. D. (2011). Stage structure alters how complexity affects stability of ecological networks. *Ecology Letters*, 14:75–79.

San Martin, E., Irigoien, X., Harris, R. P., López-Urrutia, Á., Zubkov, M. Z., and Heywood, J. L. (2006). Variation in the transfer of energy in marine plankton along a productivity gradient in the Atlantic Ocean. *Limnology and Oceanography*, 51:2084–2091.

Santos, M. N., Gaspar, M. B., Vasconcelos, P., and Monteiro, C. C. (2002). Weight-length relationships for 50 selected fish species of the Algarve coast (southern Portugal). *Fisheries Research*, 59:289–295.

Sharpe, D. M. T. and Hendry, A. P. (2009). Life history change in commercially exploited fish stocks: an analysis of trends across studies. *Evolutionary Applications*, 2:260–275.

Sheldon, R., Prakash, A., and Sutcliffe Jr., W. H. (1972). The size distribution of particles in the ocean. *Limnology and Oceanography*, 17:327–340.

693 Sheldon, R. W. and Parsons, T. R. (1967). A continuous size spectrum for particulate matter
694 in the sea. *Journal of the Fisheries Research Board Canada*, 24:909–915.

695 Shin, Y.-J. and Cury, P. (2004). Using an individual-based model of fish assemblages to
696 study the response of size spectra to changes in fishing. *Canadian Journal of Fisheries and*
697 *Aquatic Sciences*, 61:414–431.

698 Silvert, W. and Platt, T. (1978). Energy flux in the pelagic ecosystem: a time-dependent
699 equation. *Limnology and Oceanography*, 23:813–816.

700 Smith, C. and Reay, P. (1991). Cannibalism in teleost fish. *Reviews in Fish Biology and*
701 *Fisheries*, 1:41–64.

702 Speirs, D. C., Guirey, E. J., Gurney, W. S. C., and Heath, M. R. (2010). A length-structured
703 partial ecosystem model for cod in the North sea. *Fisheries Research*, 106:474–494.

704 Ursin, E. (1973). On the prey size preferences of cod and dab. *Meddelelser fra Danmarks*
705 *Fiskeri- og Havundersogelser*, 7:85–98.

706 van Denderen, P. D. and van Kooten, T. (2013). Size-based species interactions shape herring
707 and cod population dynamics in the face of exploitation. *Ecosphere*, 4:130.

708 van Kooten, T., de Roos, A. M., and Persson, L. (2005). Bistability and an Allee effect as
709 emergent consequences of stage-specific predation. *Journal of Theoretical Biology*, 237:67–
710 74.

711 Villamor, B., Abaunza, P., and Fariña, A. C. (2004). Growth variability of mackerel (*Scomber*
712 *scombrus*) off north and northwest Spain and a comparative review of the growth patterns
713 in the northeast Atlantic. *Fisheries Research*, 69:107–121.

714 Walters, C., Christensen, V., and Pauly, D. (1997). Structuring dynamic models of exploited
715 ecosystems from trophic mass-balance assessments. *Reviews in Fish Biology and Fisheries*,
716 7:139–172.

717 Ware, D. M. (1978). Bioenergetics of pelagic fish: theoretical change in swimming speed and
718 ration with body size. *Journal of the Fisheries Research Board Canada*, 35:220–228.

719 Werner, E. E. and Gilliam, J. F. (1984). The ontogenetic niche and species interactions in
720 size-structured populations. *Annual review of Ecology and Systematics*, 15:393–425.

721 Zhou, S., Smith, A. D. M., Punt, A. E., Richardson, A. J., Gibbs, M., Fulton, E. A., Pascoe,
722 S., Bulman, C., Bayliss, P., and Sainsbury, K. (2010). Ecosystem-based fisheries man-
723 agement requires a change to the selective fishing philosophy. *Proceedings of the National*
724 *Acadmy of Sciences*, 107:9485–9489.

Table 1: Model parameters and values.

Parameter	mackerel	cod	Unit	Comments
				Fish life histories:
$w_0 e^{x_{i,0}}$	0.001	0.001	g	mass of fish egg
$w_0 e^{x_{i,m}}$	200	2000	g	mass at 50% maturity
$w_0 e^{x_{i,\infty}}$	650	30000	g	asymptotic mass
$\rho_{i,m}$	15	8	–	controls the body-size range over which maturation occurs
ρ	0.2	0.2	–	exponent for approach to asymptotic body size in reproduction funcion
				Dynamic size spectra of fish species:
K	0.2	0.2	–	food conversion efficiency
α_i	0.8	0.8	–	search rate scaling exponent
A_i	750	700	$\mathrm{m}^3\ \mathrm{y}^{-1}\mathrm{g}^{-\alpha}$	feeding rate constant
β_i	6	4.5	–	natural log of mean predator prey mass ratio
σ_i	2.5	1.9	–	diet breadth
$\theta_{i,0}, \theta_{i,1}, \theta_{i,2}$	1	1	–	predator preferences for prey types 0, 1, 2
$\mu_{o,i}^{(0)}$	0.1	0.1	y^{-1}	intrinsic (non-predation) mortality rate at birth
ξ	-0.15	-0.15	–	exponent for intrinsic (non-predation) mortality
				Fixed plankton size spectrum:
$w_0 e^{x_{0,min}}$	4.8×10^{-11}		g	lowest body mass of plankton
$w_0 e^{x_{0,max}}$	0.03		g	greatest body mass of plankton
$u_{0,0}$	100		m^{-3}	plankton density at 1 mg
γ	2		–	exponent of plankton spectrum

Figure legends

Figure 1: Equilibrium properties of an unexploited ecosystem, with parameters as in Table 1. Heavy lines are for coexisting mackerel and cod; thin lines are for systems with a single species. Continuous lines refer to the left-hand vertical axes, and dashed lines to the right-hand axes. The dotted lines in (e) and (f) are von Bertalanffy growth curves for mackerel (Villamor et al., 2004) and cod (Limburg et al., 2008).

Figure 2: Mass flows at equilibrium for the unexploited ecosystem in Fig. 1 (units: g m^{-3} y^{-1}). The calculation was done without the diffusion term of the dynamical system, with $dx = 0.025$. See Eq. (2.3) *et seq.* for notation.

Figure 3: Equilibrium biomasses (thick lines) and yields (thin lines) in fisheries with fishing mortality F fixed for one species, and variable for the other. Continuous lines: mackerel; dashed lines: cod. Fishing mortality rates are: (a) variable mackerel F_m, fixed cod $F_c = 0.5$ y^{-1} ; (b) variable cod F_c, fixed mackerel $F_m = 1.0$ y^{-1}. Other parameters as in Table 1.

Figure 4: Equilibrium yields in a size-at-entry fishery with balancing between species; mackerel: filled circles; cod: open circles. Dashed lines are lines of constant exploitation rate: 0.01, 0.02, 0.04, 0.06, 0.08, 0.1, 0.5, 1.0, with exploitation rate increasing moving up the figures. (a) Fishing mortality retaining the same ratio Y_i/P_i in each species, up to collapse of cod. (b) Fishing mortality set in proportion to productivity P_i of each species. Other parameters as in Table 1.

Figure 5: Equilibrium yields with balancing across species and over body sizes within species; mackerel: filled circles; cod: open circles. Dashed lines are lines of constant exploitation rate: 0.01, 0.05, 0.1, 0.5, 1.0, with exploitation rate increasing moving up the figures. (a) Fishing mortality balanced by mass-specific growth rate, $g_i(x)$ of each species and each body size within species, and increased up to collapse of cod. (b) Fishing mortality balanced by productivity of each species and each body size within species. Other parameters as in Table 1.

Figure 6: Equilibrium size spectra of mackerel (dotted) and cod (continuous) under contrasting patterns of harvesting (heavy) and in the absence of exploitation (light). Total biomass

(mackerel+cod) at harvested equilibria is approximately 0.75 of the unexploited ecosystem. (a) Balancing across species in a size-at-entry fishery (Fig. 4b); $F_m = 2.17$, $F_c = 0.66\ \mathrm{y}^{-1}$. (b) Balancing across body size and species (Fig. 5b); constant c_4 that weights the productivity at each body size for generating size-specific fishing rates is 7.0 $\mathrm{m}^3\ \mathrm{g}^{-1}$. Other parameters as in Table 1.

Figure 7: Stability of exploited ecosystems at equilibrium under contrasting patterns of harvesting. Conventional size-at-age fishery (continuous), size-at-entry with balancing across species (dashed), balancing across body size and species (dotted). Fishing mortalities defined in the text; other parameters as in Table 1. The upper two lines are terminated at the point where cod was eliminated; mackerel and cod coexisted over the full range of fishing in the lowest line. Y_i/B_i gives a comparable measure of the average fishing mortality for different kinds of harvesting. The real part of the leading eigenvalue λ measures the time course of small perturbations from equilibrium, the return to equilibrium becoming slower as the eigenvalue approaches zero from a negative value, and not returning at all when positive.

Figure 8: Survivorships computed under the conditions of Fig. 6, for (a) mackerel, and (b) cod. Survivorships in unexploited ecosystem (continuous), size-at entry fishery with balancing across species (dashed), full balancing across body size and species (dotted). Parameter values as in Fig. 6.

Figure 9: Cohort biomass (heavy lines) in the equilibrium, unexploited ecosystem in Fig. 1 for: (a) mackerel, (b) cod, computed as the product of body mass and proportion surviving from age 0 to each age. The somatic growth rates (dotted lines) and total death rates (dashed lines) are included to show that extrema of cohort biomasses occur at the intersections of the rate lines. Note the resemblance of these cohort biomasses to the productivities in Fig. 1c, d.

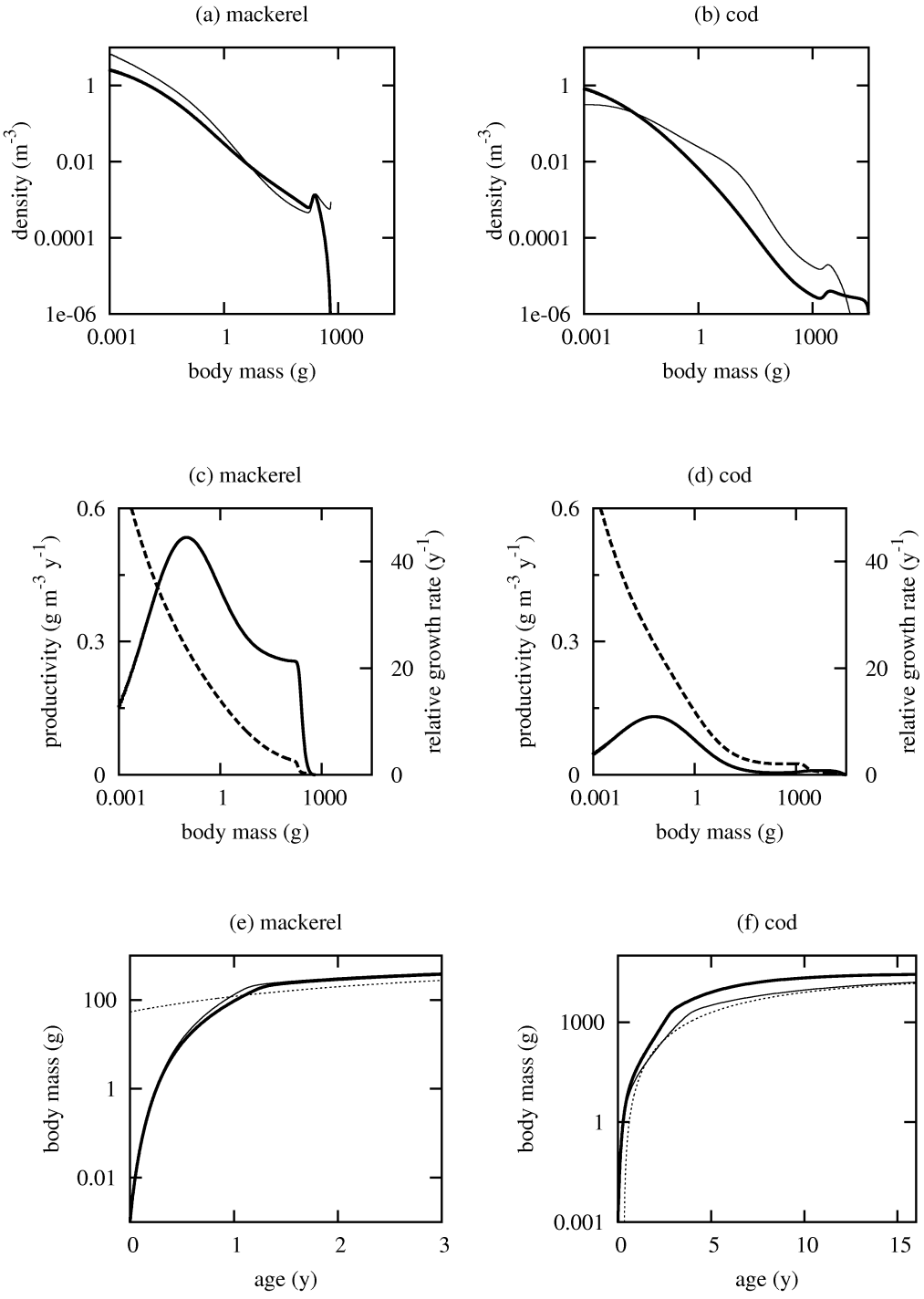
(a) mackerel
density (m-3)
1
0.01
0.0001
1e-06
0.001
1
1000
body mass (g)
(b) cod
density (m-3)
1
0.01
0.0001
1e-06
0.001
1
1000
body mass (g)
(c) mackerel
productivity (g m-3 y-1)
0.6
0.3
0
40
20
0
relative growth rate (y-1)
0.001
1
1000
body mass (g)
(d) cod
productivity (g m-3 y-1)
0.6
0.3
0
40
20
0
relative growth rate (y-1)
0.001
1
1000
body mass (g)
(e) mackerel
body mass (g)
100
1
0.01
0
1
2
3
age (y)
(f) cod
body mass (g)
1000
1
0.001
0
5
10
15
age (y)

Figure 1:

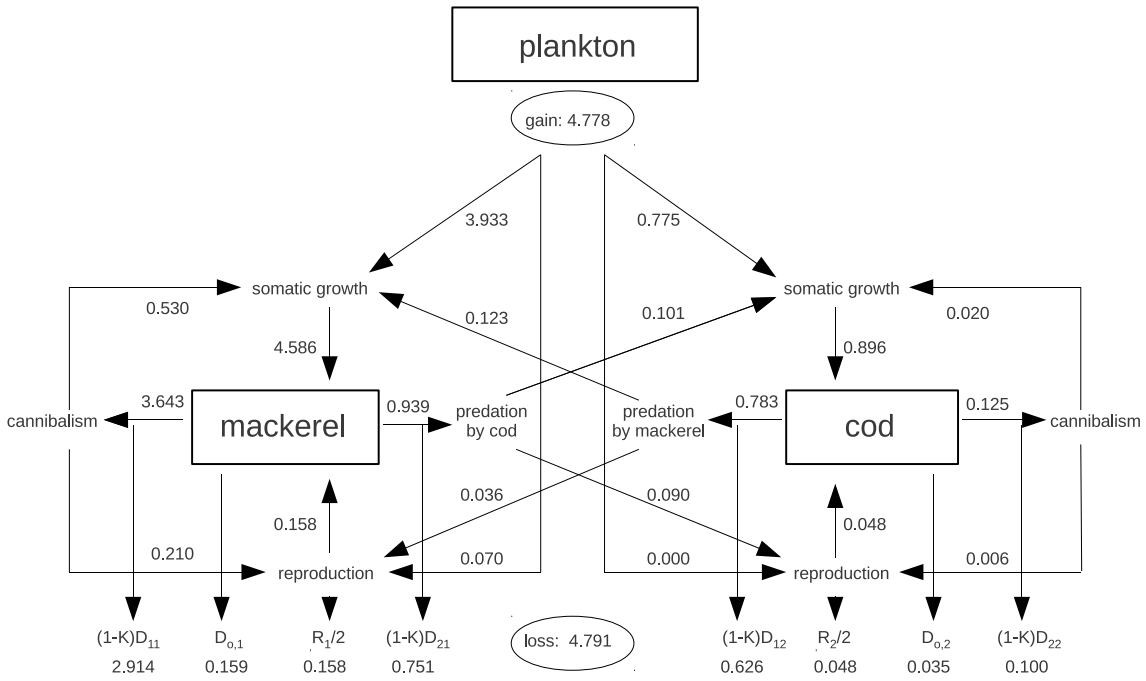
plankton
gain: 4.778
3.933
0.775
somatic growth
somatic growth
0.530
0.123
0.101
0.020
4.586
0.896
cannibalism
3.643
mackerel
0.939
predation by cod
predation by mackerel
0.783
cod
0.125
cannibalism
0.036
0.090
0.158
0.048
0.210
reproduction
0.070
0.000
reproduction
0.006
(1-K)D11
2.914
Do,1
0.159
R1/2
0.158
(1-K)D21
0.751
loss: 4.791
(1-K)D12
0.626
R2/2
0.048
Do,2
0.035
(1-K)D22
0.100

Figure 2:

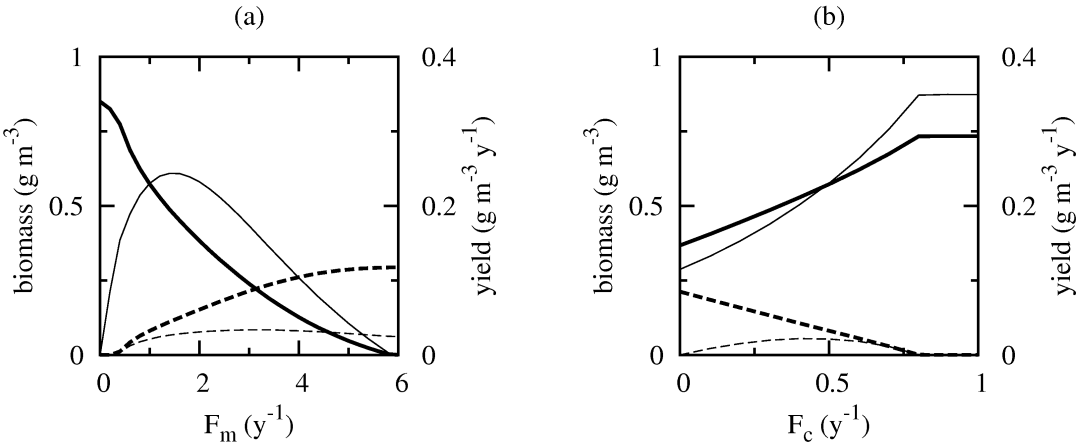

Figure 3:

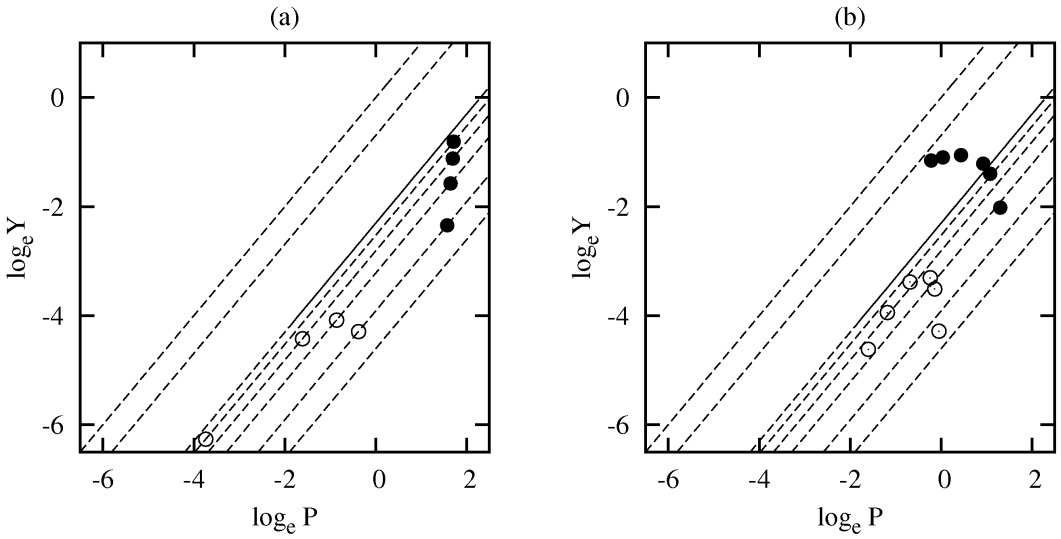

Figure 4:

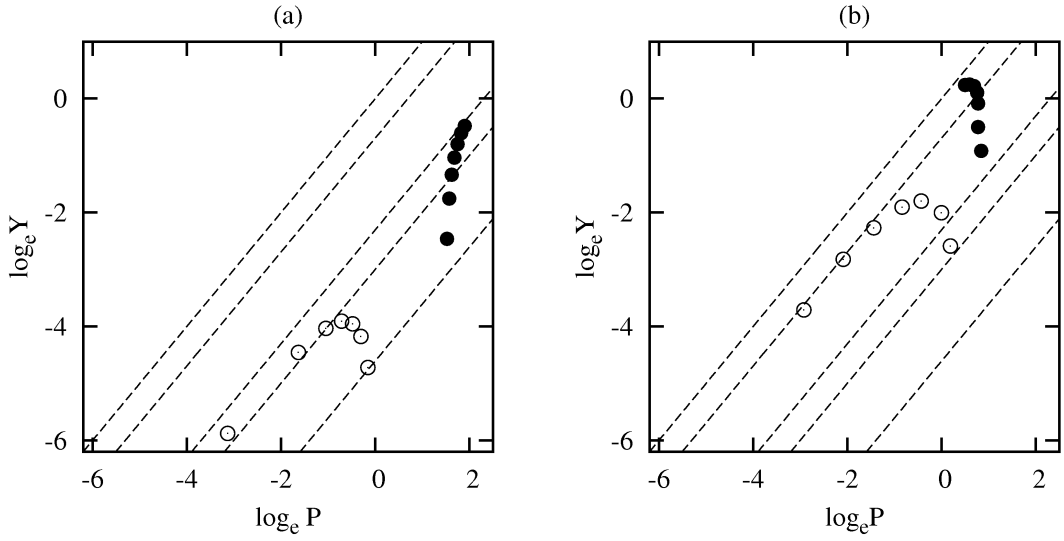

Figure 5:

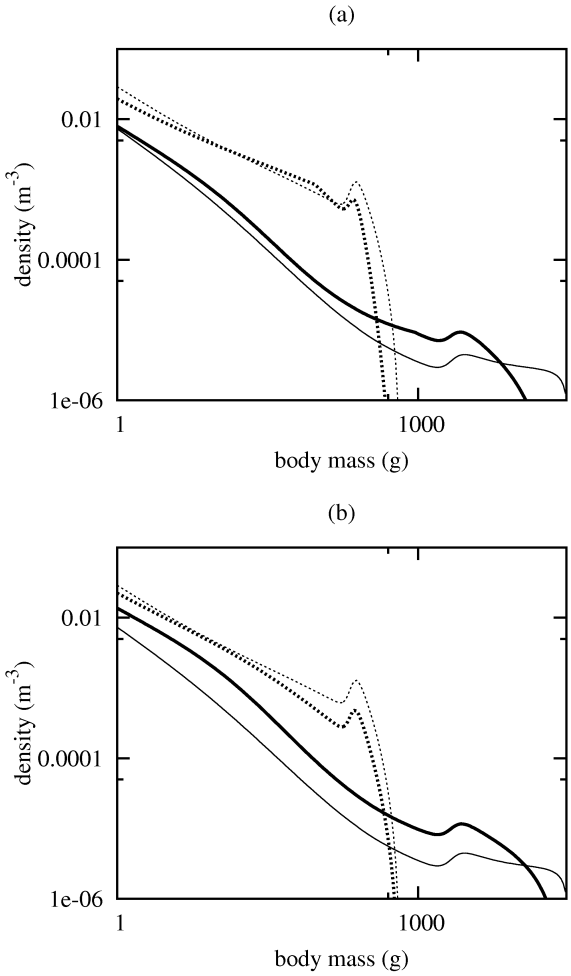
(a)
0.01
0.0001
1e-06
density (m-3)
1
1000
body mass (g)
(b)
0.01
0.0001
1e-06
density (m-3)
1
1000
body mass (g)

Figure 6:

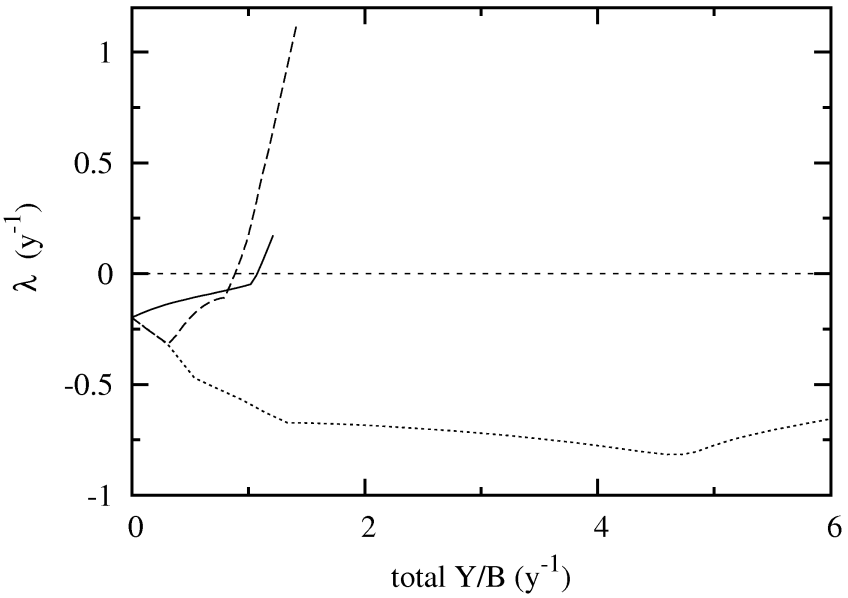

Figure 7:

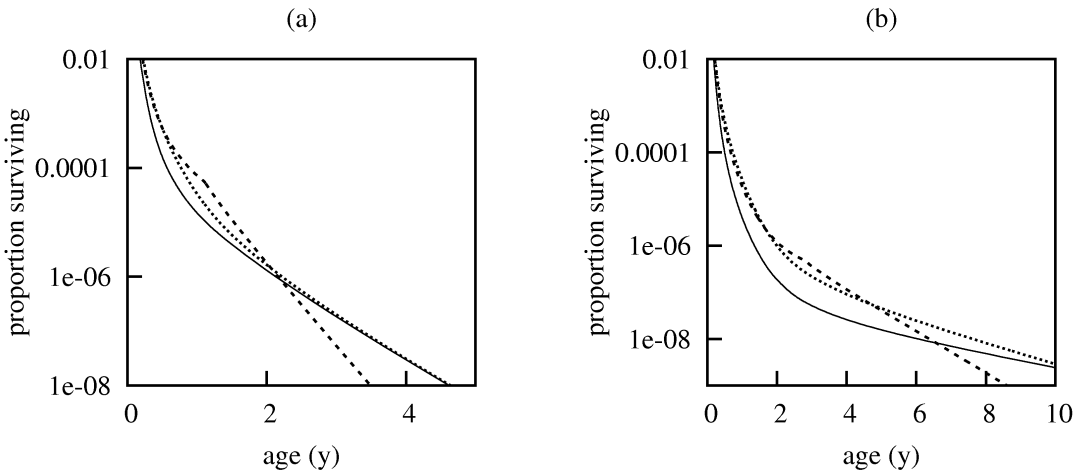

Figure 8:

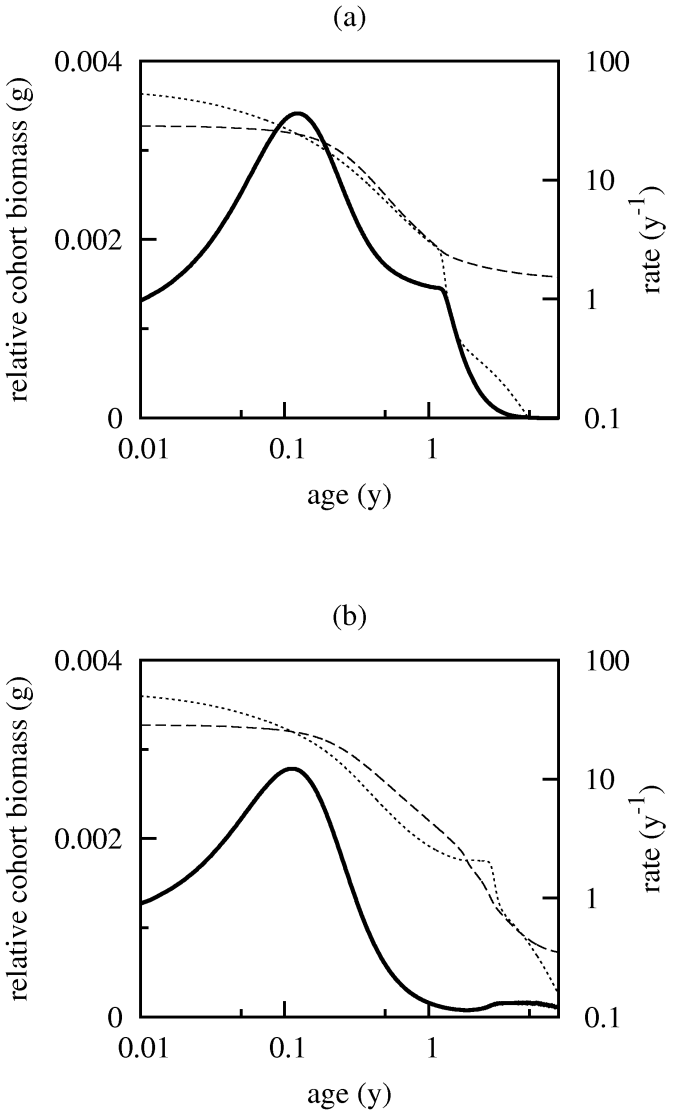
(a)
0.004
0.002
0
relative cohort biomass (g)
100
10
1
0.1
rate (y-1)
0.01
0.1
1
age (y)
(b)
0.004
0.002
0
relative cohort biomass (g)
100
10
1
0.1
rate (y-1)
0.01
0.1
1
age (y)

Figure 9:

Appendices

A Multispecies dynamics

Working from the basic jump-growth equation (Datta et al., 2010), the rate of change of density $\phi_i(w)$ of species i at mass w is partitioned into the following components:

$$\begin{aligned}\frac{\partial}{\partial t}\phi_i(w) = \int \sum_{j=0}^{n} \Bigg(& - \overbrace{\epsilon_i(w) T_{ij}(w, w') \phi_i(w) \phi_j(w')}^{\text{growth to larger size}} \\ & - \overbrace{T_{ji}(w', w) \phi_j(w') \phi_i(w)}^{\text{death due to predation}} \\ & + \overbrace{\epsilon_i(w - Kw') T_{ij}(w - Kw', w') \phi_i(w - Kw') \phi_j(w')}^{\text{growth from smaller size}} \Bigg) dw' \\ & + \overbrace{\frac{b_i(w) R_i}{2w_i}}^{\text{reproduction}} - \overbrace{(\mu_{o,i}(w) + \mu_{f,i}(w)) \phi_i(w).}^{\text{non-predation mortality}} \end{aligned} \tag{A.1}$$

where predation acts over all components in an ecosystem comprising n fish species $j = 1, \ldots, n$, and plankton, denoted by the index 0. All functions involving predation depend on time t, but this is suppressed for notational simplicity. For simplicity the plankton spectrum is assumed to be fixed, leaving a system of n integro-differential equations, $i = 1, \ldots, n$, one equation for each fish species. Eq. (A.1) is not identical to previous versions of the jump-growth equation with reproduction (Law et al., 2012, 2013). We have made the change so that biomass is fully accounted for.

In Eq. (A.1), the function $T_{ij}(w_1, w_2)$ describes the rate at which predators of mass w_1 in species i feed on prey of mass w_2 in taxon j. The function $\epsilon_i(w)$ is the proportion of predators of species i at mass w that allocate the incoming mass of prey to somatic growth as opposed to reproduction; this encodes some basic information about the species' life-history, and increases to a value 1 at the maximum body size of species i. K is the food

conversion efficiency. The function $\mu_{o,i}(w)$ is species i's per capita mortality rate at mass w due to natural causes other than predation, and $\mu_{f,i}(w)$ is the fishing mortality rate on i at mass w. R_i is the total mass rate at which reproductive biomass is created in species i:

$$R_i = K \int \big(1 - \epsilon_i(w)\big)\phi_i(w) \left(\int \sum_{j=0} T_{ij}(w, w')\phi_j(w')w' dw' \right) dw, \tag{A.2}$$

and the factor 1/2 in Eq. (A.1) allows for half of the mass being lost through males. The mass of an egg is distributed as a birth kernel $b_i(w)$, normalized to sum to 1, here assumed to be a Dirac-δ function corresponding to a single egg size $w_{i,0}$ for species i.

Taking a Taylor expansion around w of terms in the "growth-into-w" expression in Eq. (A.1), gives

$$\begin{aligned} &+ \quad (Kw')^0 \epsilon_i(w) T_{ij}(w, w')\phi_i(w)\phi_j(w') \\ &- \quad (Kw')^1 \frac{\partial}{\partial w}\Big[\epsilon_i(w) T_{ij}(w, w')\phi_i(w)\phi_j(w')\Big] \\ &+ \quad \frac{(Kw')^2}{2}\frac{\partial^2}{\partial w^2}\Big[\epsilon_i(w) T_{ij}(w, w')\phi_i(w)\phi_j(w')\Big] + O(K^3). \end{aligned} \tag{A.3}$$

This expression is substituted into Eq. (A.1). Then a logarithmic transformation $x = \ln(w/w_0)$ of body mass is introduced, where w_0 is an arbitrary body mass. This gives a new state variable $u_i(x)dx = \phi_i(w)dw$ with dimensions L^{-3} (Benoît and Rochet, 2004), and the dynamics of $u_i(x)$ are given by the partial differential equation

$$\frac{\partial}{\partial t}u_i = -\frac{\partial}{\partial x}\big[\epsilon_i g_i u_i\big] + \frac{1}{2}\frac{\partial}{\partial x}\Big[e^{-x}\frac{\partial}{\partial x}\big[\epsilon_i G_i u_i\big]\Big] + \frac{\hat{b}_i \hat{R}_i}{2}e^{-x} - \big(\mu_i + \mu_{o,i} + \mu_{f,i}\big)u_i + O(K^3), \tag{A.4}$$

where the argument x has been omitted from each function, and $\hat{b}_i(x)dx = b_i(w)dw$, $\hat{R}_i = R_i/w_0$. We include terms up to second order here, going a step beyond the approximation of the size-based McKendrick–von Foerster equation (Datta et al., 2010, 2011). The numerical results in this paper are based on this equation.

Some extra information about the feeding rate T_{ij} is introduced (Benoît and Rochet, 2004;

Andersen and Beyer, 2006; Datta et al., 2010) so that, after transformation,

$$T_{ij}(x, x') = A_i e^{\alpha_i x} s_i(e^{x-x'})\theta_{ij}. \tag{A.5}$$

Here the volume searched per unit time by a predator of species i at size x is written as $A_i e^{\alpha_i x}$, to make it scale with body size (Ware, 1978). The term $s_i(e^{x-x'})$ is a dimensionless feeding kernel for predator species i, dependent on the predator-prey mass ratio $w/w' = e^{x-x'}$ (Ursin, 1973), and we assume that $s_i(e^{x-x'}) = 0$ if $x' > x$, on the grounds that predators are typically larger than their prey. The dimensionless parameter θ_{ij} is the preference of i for prey of type j relative to prey of type i (Hartvig et al., 2011). Thus $\theta_{ij} = 1$, if predation is indiscriminate across prey species. Alternatively, it could have a smaller value to allow for, say, spatial separation of j from i that makes encounters with j relatively rare. If i does not encounter j, $\theta_{ij} = 0$,.

Using Eq. (A.5) in Eq. (A.4), the function $\mu_i(x)$ is the per capita death rate of species i at size x, due to predation by all fish species

$$\mu_i(x) = \sum_{j=1}^{n} A_j \theta_{ji} \int e^{\alpha_j x'} s_j(e^{x'-x}) u_j(x') dx'. \tag{A.6}$$

The function $g_i(x)$ is the mass specific growth rate of species i at size x from eating prey of all taxa, before partitioning it between somatic growth and reproduction

$$g_i(x) = A_i K e^{(\alpha_i - 1)x} \sum_{j=0}^{n} \theta_{ij} \int e^{x'} s_i(e^{x-x'}) u_j(x') dx'. \tag{A.7}$$

$G_i(x)$ is the corresponding rate function for the second-order diffusion term

$$G_i(x) = A_i K^2 e^{(\alpha_i - 1)x} \sum_{j=0}^{n} \theta_{ij} \int e^{2x'} s_i(e^{x-x'}) u_j(x') dx'. \tag{A.8}$$

The intrinsic mortality rate $\mu_{o,i}(x)$ accounts for sources of mortality other than predation and fishing. We assume that this is proportional to the mass-specific needs for metabolism, relative to the mass-specific rate at which food becomes available at size x. These rates are

set relative to their values at egg size, so $\mu_{o,i}(x_{i,0}) = \mu_{o,i}^{(0)}$ is a fixed baseline intrinsic mortality at birth for species i. The metabolic need should scale with body mass, and we write this as $\exp(-\xi(x - x_{i,0}))$, using the same exponent for all species. The mass specific rate of food intake at size x relative to size $x_{i,0}$ is $g_i(x)/g_i(x_{i,0})$. Thus

$$\mu_{o,i}(x) = \mu_{o,i}^{(0)} \exp(-\xi(x - x_{i,0}))g_i(x_{i,0})/g_i(x), \tag{A.9}$$

which is also a function of time because it depends on the mass-specific growth rate $g_i(x)$.

The function $\epsilon_i(x)$ is defined in terms of allocation of incoming mass to reproduction, using a form suggested by Hartvig et al. (2011):

$$1 - \epsilon_i(x) = \Big[1 + \exp(-\rho_{i,m}(x - x_{i,m}))\Big]^{-1} \exp(\rho(x - x_{i,\infty})). \tag{A.10}$$

Here $w_0 e^{x_{i,m}}$ is the body mass at which 50 % of the fish of species i are mature, and $\rho_{i,m}$ defines the body-mass range over which fish are maturing. The asymptotic body mass $w_0 e^{x_{i,\infty}}$ is the size at which all incoming mass is allocated to reproduction and no further somatic growth is possible, the approach to this size being scaled by a parameter ρ common to all species.

The egg size $x_{i,0}$ and asymptotic size $x_{i,\infty}$ together give boundary conditions for Eq. (A.4), over which there is no flux of individuals. In other words, individuals cannot grow from size $x_i < x_{i,0}$ to $x_i > x_{i,0}$ nor shrink from size $x_i > x_{i,0}$ to $x_i < x_{i,0}$, with a similar condition at the upper boundary. Mathematically, these boundary conditions are written as follows

$$J(x_{i,0}) = J(x_{i,\infty}) = 0, \tag{A.11}$$

where the flux J is the sum of the advective and diffusive fluxes in Eq. (A.4):

$$J(x) = \epsilon_i(x) g_i(x) u_i(x) - \frac{1}{2} e^{-x} \frac{\partial}{\partial x}(\epsilon_i(x) G_i(x) u_i(x)). \tag{A.12}$$

For simplicity, we do not deal with the dynamics of the plankton. This can be thought

of as an assumption that the plankton operate on a short time scale relative to the fish community. For instance, if a semi-chemostat model is used

$$\frac{\partial}{\partial t}u_0(x,t) = \frac{1}{\tau}(f(x) - u_0(x,t)) - \text{predation}, \tag{A.13}$$

there is a limit at $\tau = 0$ in which $u_0(x,t) = f(x)$ for all t, equivalent to our model. The fixed plankton spectrum was taken as $u_0(x) = f(x) = u_{0,0}\exp^{(1-\gamma)x}$, where $u_{0,0}$ is the plankton abundance at 1 mg, giving a power-law relationship between body mass and abundance.

B Numerics

Parameter values were set to match approximately the life histories of mackerel and cod.

Mackerel egg mass was obtained from a diameter 1.24 mm (Mendiola et al., 2006) and specific gravity 1.02 (Coombs, 1981), giving a mass 0.8 mg, which we rounded to 1 mg. Maturation occurs around age 2 y, when body mass is approximately 200 g (ICES, 2013a); we therefore took the body size at which 50 % of individuals are mature as 200 g. With a value $\rho_{1,m} = 15$, maturation was starting at approximately 170 g. Villamor et al. (2004) give average parameters for the von Bertalanffy growth equation of mackerel as $L_\infty = 42.7$ cm, $k = 0.268$ y^{-1}, and $t_0 = -2.17$ y. To convert from length l (cm) to mass w (g), we used an allometric relation $w = 0.0064l^{3.079}$ (Santos et al., 2002), giving an approximate asymptotic mass of 650 g. The von Bertalanffy growth equation is unable to fit mackerel's fast growth in its first year, and has to make t_0 strongly negative. This issue does not arise in the growth trajectory of the size-spectrum model, if the volumetric search-rate parameter A_i is made sufficiently large (Hunter, 1981); we set this at 750 m^3 y^{-1} g$^{-\alpha}$, in contrast to a value 600 in Law et al. (2012, 2013). The feeding kernel of mackerel was centred on a predator:prey body size ratio 400:1 ($\beta = 6$); this weights mackerel towards a planktivorous habit relative to cod (Olaso et al., 2005), the majority of its diet being in the size range of plankton until a body mass of approximately 10 g is reached. For simplicity, the diet breadth parameter σ was set at 2.5; a significantly smaller value would have destabilized the

single-species mackerel subsystem, creating a more complicated periodic solution. There was no discrimination between prey taxa at a given prey size, i.e. $\theta_{1,0} = \theta_{1,1} = \theta_{1,2} = 1$.

Cod egg mass was obtained from an average diameter of 1.6 mm (Chambers and Waiwood, 1996) and an assumption of neutral buoyancy, to give an average egg mass of 1.6 mg, which we rounded to 1 mg. We took a value for 50 % maturity at 2 kg, and an asymptotic mass at 30 kg (Bogstad, personal communication). With a value $\rho_{2,m} = 8$, maturation was starting at approximately 1.5 kg. Limburg et al. (2008) (Supplement) give average von Bertalanffy parameters for Baltic cod in 1995 as $L_\infty = 137.6$ cm, $k = 0.1223$ y^{-1}, and $t_0 = 0.3115$ y, and we use an allometric relation $w = 0.009l^{3.00}$ for conversion to mass (Bogstad, personal communication). We set the food searching parameter A_i for cod somewhat smaller than that for mackerel, at 700 m^3 y^{-1} g$^{-\alpha}$, to match its slower growth when small. The feeding kernel of cod was centred on a predator:prey body size ratio 90:1 ($\beta = 4.5$), with a diet breadth $\sigma = 1.9$, based on information from Georges Bank cod given in Table 4.1 of Blanchard (2008). There was no discrimination between prey taxa at a given prey size, i.e. $\theta_{2,0} = \theta_{2,1} = \theta_{2,2} = 1$.

In setting parameter values for the intrinsic mortality rate $\mu_{o,i}(x)$, we note that metabolic rate is unlikely to scale with body size with an exponent -0.25 in fish (equivalent to +0.75 per individual of Kleiber's law). Killen et al. (2007) reported exponents for standard metabolic rate in three species of fish around -0.17, rising to around -0.1 as metabolic activity increased in keeping with a broader meta-analysis of ectotherms (Glazier, 2009) (we have made the transformation to mass-specific scalings here by subtracting 1). We therefore assumed a value $\xi = -0.15$. A low value $\mu_{o,i}^{(0)} = 0.1$ y^{-1} was used for for the intrinsic mortality rate at birth for both species, so that most mortality would come from predation.

The lower limit of body size for the plankton was set at $\exp(-20)$ of the fish egg mass. i.e. 4.8×10^{-11} g, to ensure a good coverage for the mackerel feeding kernel for the smallest larvae, and we allowed some overlap of the plankton spectrum with the fish spectra by setting the upper size limit at 0.03 g. We set the density of plankton at 1 mg, $u_{0,0}$, to a value 100 m^{-3}, based on interpolation from San Martin et al. (2006, Figure 2c), and took the standard assumption that abundance scales with body mass with an exponent $\gamma = 2$ (San Martin et al., 2006).

Numerical computation of the steady state was done in two steps. First, a numerical integration of Eq. (A.4) was carried out to get near to the steady state (in some cases the steady state was not an attractor). Then a Newton-Raphson algorithm was used to solve for the steady state and to obtain information on its local asymptotic stability through the eigenvalues of the Jacobian matrix. The stability of dynamic size spectra is sensitive to the discretization of body mass, so we used as small a step size as possible. This was $dx = 0.05$ unless otherwise stated.

C Mass balance at steady state

Consider the steady state at which the right-hand side of Eq. (A.4) is zero, writing the steady-state density for species i as $\hat{u}_i(x)$. We include terms in Eq. (A.4) up to first order. It is possible to include second-order terms and this results in a slightly modified expression for the total productivity P_i of species i; numerically this makes a negligible difference to the value of P_i. Multiplying Eq. (A.4) through by the body mass $w_0 e^x$ and integrating from $x = x_{i,0}$ to $x = x_{i,\max}$ gives:

$$0 = -\int w_0 e^x (\mu_i + \mu_{o,i} + \mu_{f,i}) u_i dx - \int w_0 e^x \frac{d}{dx}(\epsilon_i g_i u_i) dx + \int w_0 \frac{\hat{R}_i \hat{b}_i}{2} dx \qquad \text{(C.1)}$$

We retain w_0 in these expressions so that the mass flows all have the standard dimensions (M L^{-3} T^{-1}). The first integral in this equation is the total rate at which biomass is being lost from species i due to mortality. This can be decomposed into the rate of biomass loss to predation mortality, which we write as D_i, the rate of biomass loss to intrinsic mortality, which we write as $D_{o,i}$ and rate of biomass loss to fishing mortality, which is equivalent to the yield, Y_i. Using integration by parts on the second integral and the fact that $\hat{b}_i$ is a Dirac-δ function, we have

$$0 \;=\; -D_i - D_{o,i} - Y_i - [w_0 e^x \epsilon_i g_i u_i]_{x_{i,0}}^{x_{i,\infty}} + \int w_0 e^x \epsilon_i g_i u_i dx + w_0 \frac{\hat{R}_i}{2}. \qquad \text{(C.2)}$$

The boundary conditions (A.11) mean that there is no contribution from the term $[e^x \epsilon_i g_i u_i]_{x_{i,0}}^{x_{i,\infty}}$. The remaining integral is the total rate at which biomass is being accumulated due to somatic growth of species i, i.e. the total productivity P_i. Thus the overall balance for species i at steady state is:

$$P_i + R_i/2 = D_i + D_{o,i} + Y_i. \tag{C.3}$$

The term $R_i/2$ is a net flow of mass to reproduction, after loss of the male component. So the full balance between gains and losses is:

$$P_i + R_i = D_i + D_{o,i} + Y_i + R_i/2. \tag{C.4}$$

Each term in this equation is a rate of mass flow (M L^{-3} T^{-1}) measured at the population level for species i. The terms on the left-hand side correspond to processes that generate new biomass (somatic growth and reproduction) and those on the right-hand side correspond to processes that cause loss of biomass, i.e. mortality and the contribution of males to reproduction. Terms in this equation involving predation can be disaggregated down to the mass flow corresponding to each prey or predator species; the totals used above are the sum of these components: $P_i = \sum_j P_{ij}$, $R_i = \sum_j R_{ij}$, and $D_i = \sum_j D_{ji}$.

For reference purposes, the general version of this that includes the diffusive terms looks like this:

$$\begin{aligned} 0 &= -\int e^x(\mu_i + \mu_{o,i} + \mu_{f,i})u_i dx - \int e^x \frac{dJ}{dx} dx + \int \frac{\hat{R}_i \hat{b}_i}{2} dx \\ &= -D_i - D_{o,i} - Y_i - w_0[e^x J]_{x_{i,0}}^{x_{i,\infty}} + w_0 \int e^x J dx + \frac{R_i}{2}, \end{aligned} \tag{C.5}$$

where J is given by Eq. (A.12). The boundary conditions (A.11) specify that $J(x_{i,0}) = J(x_{i,\infty}) = 0$, so there is no contribution from the boundary term. The productivity is given by the remaining integral, $\int e^x J dx$, as this is the net rate of biomass accumulation for species i, summed over all body sizes. We therefore have the same mass balance equation as

previously, Eq. (C.4), but with a different expression for the productivity:

$$\begin{aligned} P_i &= w_0 \int e^x J dx \\ &= w_0 \int e^x \left(\epsilon_i g_i u_i - \frac{1}{2} e^{-x} \frac{d}{dx} (\epsilon_i G_i u_i) \right) dx \\ &= w_0 \int e^x \epsilon_i g_i u_i dx - \frac{w_0}{2} \left[\epsilon_i G_i u_i \right]_{x_{i,0}}^{x_{i,\infty}} \\ &= w_0 \int e^x \epsilon_i g_i u_i dx + \frac{w_0}{2} G_i(x_{i,0}) u_i(x_{i,0}), \end{aligned} \tag{C.6}$$

where the last line results from the fact that $\epsilon_i(x_{i,\infty}) = 0$ and $\epsilon_i(x_{i,0}) = 1$. Numerically, the "correction term" $G_i(x_{i,0})u_i(x_{i,0})w_0/2$ is very small ($< 0.1\%$) compared to the main integral term.

D Multispecies harvesting

Yields Y_i, from harvesting species i in a multispecies ecosystem are based on the equation:

$$Y_i = \int w_0 e^x \mu_{f,i}(x) u_i(x) dx, \tag{D.1}$$

where fishing mortality $\mu_{f,i}(x)$ is set to an appropriate pattern of fishing over body size x, as required. We use the following patterns of fishing mortality.

- **Figure 3.** For a size-at-entry fishery, a simple assumption is that $\mu_{f,i}(x) = F_i$, once fish of species i have grown to the minimum size of fishing $\underline{x}_i$. Then the yield is:

$$Y_i = F_i \int_{\underline{x}_i}^{\overline{x}_i} w_0 e^x u_i(x) dx = F_i B_i^*, \tag{D.2}$$

  where B_i^* is the stock biomass integrated from the size-at-entry to the maximum size $\overline{x}_i$.

- **Figure 4a.** A size-at-entry fishery can be balanced by choosing the F_is so that both species have the same value of Y_i/P_i. Using Eq. (D.2), this is achieved by setting fishing mortality from the size-at-entry onwards as

$$\mu_{f,i}(x) = F_i = c_1 \frac{P_i}{B_i^*}, \tag{D.3}$$

  where c_1 is the constant of proportionality, and P_i is the productivity from somatic growth, as given in Eq. (C.4).

- **Figure 4b.** An alternative way of balancing a size-at-entry fishery is to weight the fishing mortality by its productivity under the current exploitation:

$$\mu_{f,i}(x) = F_i = c_2 P_i, \tag{D.4}$$

  where c_2 is a constant of proportionality that can be altered to change the overall intensity of fishing.

- **Figure 5a.** A simple way to balance size-specific harvesting to a component of productivity is to make fishing proportional to the mass-specific, somatic, growth rate:

$$\mu_{f,i}(x) = c_3 \epsilon_i(x) g_i(x), \tag{D.5}$$

  where c_3 is a constant of proportionality that remains the same across all harvested sizes of all species, but that can be altered to change the overall intensity of fishing. This has the effect of ensuring that all species have the same value of Y_i/P_i^*, because

$$\frac{Y_i}{P_i^*} = \frac{\int_{\underline{x}_i}^{\overline{x}_i} w_0 e^x c_3 \epsilon_i(x) g_i(x) u_i(x) dx}{\int_{\underline{x}_i}^{\overline{x}_i} w_0 e^x \epsilon_i(x) g_i(x) u_i(x) dx} = c_3. \tag{D.6}$$

  Notice that the productivity P_i^* must be measured over the size range of exploitation for this result to be exact.

- **Figure 5b.** The full balancing to productivity at every body size of every species is:

$$\mu_{f,i}(x) = c_4 w_0 e^x \epsilon_i(x) g_i(x) u_i(x), \tag{D.7}$$

where c_4 is a constant of proportionality that can be altered to change the overall intensity of fishing.

Note that most of these harvest patterns use information on the current status of the exploited species, such as its productivity and biomass. We take this information from the species populations at each step of numerical integration, and as the numerical analysis searches for the steady state. The measures that provide this information are themselves functions of time, and settle to fixed values when the steady state $\hat{u}_i(x)$ is reached. All results are reported at the steady state.

E Body size maximizing productivity and cohort biomass

Consider the steady state at which the right-hand side of Eq. (A.4) is zero, writing the steady-state density for species i as $\hat{u}_i(x)$. We take the first-order terms from Eq. (A.4), leaving out the diffusion term and higher-order terms:

$$0 = -\mu_{\mathrm{tot},i}(x)\hat{u}_i(x) - \frac{\partial}{\partial x}\big[\epsilon_i(x) g_i(x) \hat{u}_i(x)\big]. \tag{E.1}$$

All mortality terms have been lumped together, so $\mu_{\mathrm{tot},i} = \mu_i + \mu_{o,i} + \mu_{f,i}$, and the reproduction term has been omitted, as this only operates at the smallest body size x_0. Dividing through by $\epsilon_i(x) g_i(x) \hat{u}_i(x)$ puts the second term into a standard form for integration, giving

$$0 = -\int_{x_{i,0}}^{x} \frac{\mu_{\mathrm{tot},i}(y)}{\epsilon_i(y) g_i(y)} dy - \Big[\ln\big[\epsilon_i(x) g_i(x) \hat{u}_i(x)\big]\Big]_{x_{i,0}}^{x}. \tag{E.2}$$

Removing the logarithm, and multiplying through by body mass $w_0 e^x$, gives

$$w_0 e^{x_0} \frac{p_i(x)}{p_i(x_{i,0}^+)} = w_0 e^x \exp\Big(-\int_{x_{i,0}}^{x} \frac{\mu_{\mathrm{tot},i}(y)}{\epsilon_i(y) g_i(y)} dy\Big), \tag{E.3}$$

where $p_i(x) = w_0 e^x \epsilon_i(x) g_i(x) \hat{u}_i(x)$ is productivity at size x and $p_i(x_{i,0}^+) = \lim_{x \downarrow x_0} p_i(x)$.

Note that the rate of change of body size with respect to age a is $dx/da = \epsilon_i(x) g_i(x)$. So the exponential term in Eq. E.3 is the proportion of individuals in a cohort surviving from birth at size $x_{i,0}$ up to age a (and size x). Multiplying the integral by $w_0 e^x$, gives the cohort biomass at age a (and size x) per newborn individual, $B_{c,i}(a)$. By this argument, we establish a proportionality between the productivity at body size x, and the cohort biomass at age a (corresponding to size x), i.e. $p_i(x) \propto B_{c,i}(a)$.

To find turning points, we differentiate $p_i(x)$ with respect to size x and set the derivative to zero:

$$0 = e^x \frac{d}{dx} \left[\epsilon_i(x) g_i(x) \hat{u}_i(x) \right] + e^x \epsilon_i(x) g_i(x) \hat{u}_i(x) \tag{E.4}$$

From Eq. (E.1), the derivative in Eq. (E.4) must equal $-\hat{u}_i(x) \mu_{\text{tot},i}(x)$. Thus, in the steady-state ecosystem, turning points for $p_i(x)$ (and hence $B_{c,i}(a)$) occur at points where $\mu_{\text{tot},i}(x) = \epsilon_i(x) g_i(x)$. In other words, there is a turning point for both $p_i(x)$ and $B_{c,i}(a(x))$ when a body size x^* is reached at which the sum of all mortality rates equals the mass-specific somatic growth rate. The turning point is a maximum if $d/dx(\mu_{\text{tot},i}) > d/dx(\epsilon_i g_i)$. Note that a turning point does not necessarily exist in a feasible range of body sizes; for instance, a power-law steady state has the same exponent for predation mortality and growth rate, in which case $d/dx(\mu_{\text{tot},i}) = dg_i/dx$ for all x. Note also that, because growth and mortality are nonlinear functions, there may be more than one turning point.